

1 **The interpretation of temperature and salinity variables in numerical**  
2 **ocean model output, and the calculation of heat fluxes and heat content**

3  
4 by

5  
6 Trevor J. McDougall<sup>1</sup>, Paul M. Barker<sup>1</sup>, Ryan M. Holmes<sup>1,2,3</sup>,  
7 Rich Pawlowicz<sup>4</sup>, Stephen M. Griffies<sup>5</sup> and Paul J. Durack<sup>6</sup>

8  
9 <sup>1</sup>School of Mathematics and Statistics,  
10 University of New South Wales, Sydney, NSW 2052, Australia

11 <sup>2</sup>Climate Change Research Centre and ARC Centre of Excellence for Climate  
12 Extremes, University of New South Wales, Sydney, NSW 2052, Australia

13 <sup>3</sup>Current affiliation: School of Geosciences, University of Sydney,  
14 Sydney, NSW 2006, Australia

15 <sup>4</sup>Dept. of Earth and Ocean Sciences, University of British Columbia,  
16 Vancouver, B.C. V6T 1Z4, Canada

17 <sup>5</sup>NOAA/Geophysical Fluid Dynamics Laboratory, and Princeton University  
18 Atmospheric and Oceanic Sciences Program, Princeton, New Jersey, USA

19 <sup>6</sup>Program for Climate Model Diagnosis and Intercomparison, Lawrence Livermore  
20 National Laboratory, Livermore, California, USA

21  
22  
23 Corresponding author email: [Trevor.McDougall@unsw.edu.au](mailto:Trevor.McDougall@unsw.edu.au)

24 Full address

25 Trevor J McDougall  
26 School of Mathematics and Statistics  
27 University of New South Wales, NSW 2052, Australia  
28 tel: +61 2 9385 3498  
29 fax: +61 2 9385 7123  
30 mob: +61 407 518 183

31 keywords ocean modelling, CMIP, ocean model intercomparison, TEOS-10,  
32 EOS-80,

33  
34 Submitted to *Geoscientific Model Development*

35 This version is dated 16<sup>th</sup> September 2021

36

37 **Abstract**

38 The international thermodynamic equation of seawater of 2010 (TEOS-10) defined the  
39 enthalpy and entropy of seawater, thus enabling the global ocean heat content to be  
40 calculated as the volume integral of the product of in situ density,  $\rho$ , and potential  
41 enthalpy,  $h^0$  (with reference sea pressure of 0 dbar). In terms of Conservative  
42 Temperature,  $\Theta$ , ocean heat content is the volume integral of  $\rho c_p^0 \Theta$ , where  $c_p^0$  is a  
43 constant "isobaric heat capacity".

44 However, many ocean models in the Coupled Model Intercomparison Project  
45 phase 6 (CMIP6) as well as all models that contributed to earlier phases, such as  
46 CMIP5, CMIP3, CMIP2 and CMIP1 used EOS-80 (Equation of State - 1980) rather than  
47 the updated TEOS-10, so the question arises of how the salinity and temperature  
48 variables in these models should be physically interpreted, with a particular focus on  
49 comparison to TEOS-10 compliant observations. In this article we address how heat  
50 content, surface heat fluxes and the meridional heat transport are best calculated using  
51 output from these models, and how these quantities should be compared with those  
52 calculated from corresponding observations. We conclude that even though a model  
53 uses the EOS-80 equation of state which expects potential temperature as its input  
54 temperature, the most appropriate interpretation of the model's temperature variable  
55 is actually Conservative Temperature. This perhaps unexpected interpretation is  
56 needed to ensure that the air-sea heat flux that leaves/arrives-in the atmosphere and  
57 sea ice models is the same as that which arrives-in/leaves the ocean model.

58 We also show that the salinity variable carried by present TEOS-10 based  
59 models is Preformed Salinity, while the salinity variable of EOS-80 based models is also  
60 proportional to Preformed Salinity. These interpretations of the salinity and  
61 temperature variables in ocean models are an update on the comprehensive Griffies et  
62 al (2016) paper that discusses the interpretation of many aspects of coupled Earth  
63 system models.

64

## 65 1. Introduction

66 Numerical ocean models simulate the ocean by calculating the acceleration of  
 67 fluid parcels in response to various forces, some of which are related to spatially-varying  
 68 density fields that affect pressure, as well as solving transport equations for the two  
 69 tracers on which density depends, namely temperature [the CMIP6 variables identified  
 70 as  $\theta$  or  $\theta_s$ ] and dissolved matter (“salinity”, [CMIP6 variable  $s_o$ ]). For  
 71 computational reasons it is useful for the numerical schemes involved to be  
 72 conservative, meaning that the amount of heat and salt in the ocean changes only due to  
 73 the area integrated fluxes of heat and salt that cross the ocean’s boundaries; in the case of  
 74 salt, this is zero. This conservative property is guaranteed for ocean models to within  
 75 computational truncation error since these numerical models are designed using finite  
 76 volume integrated tracer conservation (e.g., see Appendix F in Griffies et al 2016). It is  
 77 only by ensuring such conservation properties that scientists can reliably make use of  
 78 numerical ocean models for the long (centuries and longer) simulations required for  
 79 climate and Earth system studies.

80 However, this apparent numerical success ignores some difficult theoretical  
 81 issues with the equation set being numerically solved. Here, we are concerned with  
 82 issues related to the properties of seawater that have only recently been widely  
 83 recognized because of research resulting in the Thermodynamic Equation of Seawater  
 84 2010 (TEOS-10). These issues mean that the intercomparison of different models, and  
 85 comparison with ocean observations, needs to be undertaken with care.

86 In particular, it is widely recognized that the traditional measure of heat content  
 87 per unit mass in the ocean (with respect to an arbitrary reference state), the so-called  
 88 potential temperature, is not a conservative variable (McDougall, 2003). Hence, the time  
 89 change of potential temperature at a point in space is not determined solely by the  
 90 convergence of the potential temperature flux at that point. Furthermore, the non-  
 91 conservative nature of potential temperature means that the potential temperature of a  
 92 mixture of water masses is not the mass average of the initial potential temperatures  
 93 since potential temperature is “produced” or “destroyed” by mixing within the ocean’s  
 94 interior. This empirical fact is an inherent property of seawater (e.g., McDougall 2003,

Deleted: heat content (or its related parameter,

Deleted: ,

Deleted: )

98 Graham and McDougall 2013), and so treating potential temperature as a conservative  
99 tracer (as well as making certain other assumptions related to the modelling of heat and  
100 salt) results in contradictions, which have been built into most numerical ocean models  
101 to varying degrees.

102 These contradictions have existed since the beginning of numerical ocean  
103 modelling but have generally been ignored or overlooked because many other  
104 oceanographic and numerical factors were of greater concern. However, as global heat  
105 budgets and their imbalances are now a critical factor in understanding climate changes,  
106 it is important to examine the consequences of these assumptions, and perhaps correct  
107 them even at the cost of introducing problems elsewhere. These concerns are  
108 particularly important when heat budgets are being compared between different  
109 models, and with similar calculations made with observed conditions in the real ocean.

110 The purpose of this paper is to describe these theoretical difficulties, to estimate  
111 the magnitude of errors that result, and to make recommendations about resolving them  
112 both in current and future modelling efforts. For example, the insistence that a model's  
113 temperature variable is potential temperature involves errors in the air-sea heat flux in  
114 some areas that are as large as the mean rate of current global warming. A simple re-  
115 interpretation of the model's temperature variable overcomes this inconsistency and  
116 allows coupled climate models to conserve heat.

117 The reader who wants to skip straight to the recommendations on how the  
118 salinity and temperature outputs of CMIP models should be interpreted can go straight  
119 to section 6.

120

## 121 **2. Background**

### 122 *Thermodynamic measures of heat content*

123 It is well-known that *in situ* temperature is not a satisfactory measure of the "heat  
124 content" of a water parcel because the *in situ* temperature of a water parcel changes as  
125 the ambient pressure changes (i.e., if a water parcel is transported to a different depth  
126 [pressure] in the ocean). This change is of order 0.1°C as pressure changes 1000 dbar,  
127 and is large relative to the precision of 0.01°C required to understand deep ocean

128 circulation patterns. The utility of *in situ* temperature lies in the fact that it is easily  
129 measured with a thermometer, and that air-sea boundary heat fluxes are to some degree  
130 proportional to *in situ* temperature differences.

131 Traditionally, potential temperature has been used as an improved measure of  
132 ocean heat content. Potential temperature is defined as the temperature that a parcel  
133 would have if moved isentropically and without exchange of mass to a fixed reference  
134 pressure (usually taken to be surface atmospheric pressure), and can be calculated from  
135 measured ocean *in situ* temperatures using empirical correlation equations based on  
136 laboratory measurements. However, the enthalpy of seawater varies nonlinearly with  
137 temperature and salinity (Fig. 1) and this variation results in non-conservative behaviour  
138 under mixing (McDougall (2003), section A.17 of IOC et al. (2010)). The ocean's potential  
139 temperature is subject to internal sources and sinks – it is not conservative.

140 With the development of a Gibbs function for seawater, based on empirical fits to  
141 measurements of known thermodynamic properties (Feistel (2008), IOC et al, 2010), it  
142 became possible to apply a more rigorous theory for quasi-equilibrium thermodynamics  
143 to study heat content problems in the ocean. As a practical matter, calculations can now  
144 be made that allow for an estimate of the magnitude of non-conservative terms in the  
145 ocean circulation. By integrating over water depth these production rates can be  
146 expressed as an equivalent heat flux per unit area.

147 Non-conservation of potential temperature was found to be equivalent to a root  
148 mean square surface heat flux of about  $60 \text{ mW m}^{-2}$  (Graham and McDougall, 2013), and  
149 an average value of  $16 \text{ mW m}^{-2}$  (see below). These numbers can be compared to a  
150 present-day estimated global-warming surface heat flux imbalance of between  
151  $300 \text{ mW m}^{-2}$  and  $470 \text{ mW m}^{-2}$  (Zanna et al., 2019, von Schuckmann et al., 2020). By  
152 comparison, the globally averaged rate of increase of temperature due to the dissipation  
153 of kinetic energy is approximately  $10 \text{ mW m}^{-2}$ . These equivalent heat fluxes and  
154 subsequent similar values are gathered into Table 1 for reference. In the context of a  
155 conceptual ocean model being driven by known heat fluxes, the presence of the non-  
156 conservation of potential temperature causes SST errors seasonally in the equatorial  
157 region of about  $0.5\text{K}$  ( $0.5^\circ\text{C}$ ), while the error (in all seasons) at the outflow of the

158 Amazon is 1.8K (see section 9 of McDougall, 2003). With different boundary conditions  
 159 (such as restoring boundary conditions) the error in assuming that potential temperature is  
 160 conservative is split in different proportions, between (a) the potential temperature values  
 161 and (b) the potential temperature fluxes.

162 Unfortunately, no single alternative thermodynamic variable has been found that  
 163 is both independent of pressure, and conservative under mixing. For example, specific  
 164 entropy is produced in the ocean interior when mixing occurs, with the depth-integrated  
 165 production being equivalent to an imbalance in the air-sea heat flux of a root mean  
 166 square value of about  $500 \text{ mW m}^{-2}$  (Graham and McDougall, 2013), while, apart from the  
 167 dissipation of kinetic energy, enthalpy is conservative under mixing at constant  
 168 pressure, but enthalpy is intrinsically pressure-dependent.

169 However, it was found that a constructed variable, potential enthalpy  
 170 (McDougall, 2003), has a mean non-conservation error in the global ocean of only about  
 171  $0.3 \text{ mW m}^{-2}$  (this is the mean value of an equivalent surface heat flux, equal to the depth  
 172 integrated interior production of potential enthalpy that is additional to the production  
 173 due to the dissipation of kinetic energy (Graham and McDougall, 2013)). The potential  
 174 enthalpy,  $\tilde{h}^0$ , is the enthalpy of a water parcel after being moved adiabatically and at  
 175 constant salinity to the reference pressure 0 dbar where the temperature is equal to the  
 176 potential temperature,  $\theta$ , of the water parcel:

$$177 \quad \tilde{h}^0(S_A, \theta) = h(S_A, \theta, 0\text{dbar}). \quad (1)$$

178 In Eq. (1) the function  $h$  is the specific enthalpy of TEOS-10 (defined as a function of  
 179 Absolute Salinity, in-situ temperature and sea pressure) whereas  $\tilde{h}^0$  is the potential  
 180 enthalpy function and the over-tiddle implies that the temperature input to this  
 181 function is potential temperature,  $\theta$ . By way of comparison, the area-averaged  
 182 geothermal input of heat into the ocean bottom is about  $86 \text{ mW m}^{-2}$ , and the interior  
 183 heating of the ocean due to viscous dissipation, is equivalent to a mean surface heat flux  
 184 of about  $3 \text{ mW m}^{-2}$  (Graham and McDougall, 2013). Tailleux (personal communication,  
 185 2021) has suggested that the dissipation of kinetic energy in the ocean may be as much  
 186 as three times as large as this value, at approximately  $10 \text{ mW m}^{-2}$ . Thus we conclude  
 187 that potential enthalpy, although not a theoretically ideal conservative parameter, can be

188 treated as such for many present purposes in oceanography. If at some stage in the  
 189 future a source term were to be added to the evolution equation for Conservative  
 190 Temperature, the most important contribution would be that due to the dissipation of  
 191 kinetic energy, being a factor of ~10-30 larger than the non-conservation of Conservative  
 192 Temperature due to other diffusive contributions (namely the terms on the last two lines  
 193 of Eqn. (38) of Graham and McDougall (2013)).

194 Since potential enthalpy was not a widely understood property, a decision was  
 195 made in the development of TEOS-10 to adopt Conservative Temperature,  $\Theta$ , which has  
 196 units of temperature and is proportional to potential enthalpy:

$$197 \quad \Theta = \tilde{\Theta}(S_A, \theta) = \tilde{h}^0(S_A, \theta) / c_p^0, \quad (2)$$

198 where the proportionality constant  $c_p^0 \equiv 3991.867\,957\,119\,63 \text{ J kg}^{-1} \text{ K}^{-1}$ , was chosen so that  
 199 the average value of Conservative Temperature at the ocean surface matched that of  
 200 potential temperature. Although in hindsight other choices (e.g., with fewer significant  
 201 digits) might have been more useful, this value of  $c_p^0$  is now built into the TEOS-10  
 202 standard.

203 Note that at specific locations in the ocean, in particular at low salinities and high  
 204 temperatures,  $\Theta$  and  $\theta$  can differ by more than 1°C (Fig. 2); the difference is a strongly  
 205 nonlinear function of temperature and salinity.  $\Theta$  is, by definition, independent of  
 206 adiabatic and isohaline changes in pressure.

#### 207 *Why is potential temperature not conservative?*

208 This question is answered in sections A.17 and A.18 of the TEOS-10 Manual (IOC  
 209 et al., 2010) as well as McDougall (2003) and Graham and McDougall (2013). The answer  
 210 is that potential enthalpy referenced to the sea surface pressure,  $h^0$ , which is an (almost  
 211 totally) conservative variable in the real ocean, is not simply a linear function of  
 212 potential temperature,  $\theta$ , and Absolute Salinity,  $S_A$  (and note that both enthalpy and  
 213 entropy are unknown and unknowable up to separate linear functions of Absolute  
 214 Salinity). If potential enthalpy were a linear function of potential temperature and  
 215 Absolute Salinity then the “heat content” per unit mass of seawater could be accurately  
 216 taken to be proportional to potential temperature, and the isobaric specific heat capacity  
 217

218 at zero sea pressure would be a constant. As an example of the nonlinearity of  $\tilde{h}^0(S_A, \theta)$ ,  
 219 the isobaric specific heat at the sea surface pressure  $c_p(S_A, \theta, 0\text{dbar}) \equiv h_\theta^0$  varies by 6%  
 220 across the full range of temperatures and salinities found in the World Ocean (Fig. 1).  
 221 By way of contrast, the potential enthalpy of an ideal gas is proportional to its potential  
 222 temperature.

223 Another way of treating heat in an ocean model is to continue carrying potential  
 224 temperature as its temperature variable but to (i) use the variable isobaric heat capacity  
 225 at the sea surface to relate the air-sea heat flux to an air-sea flux of potential temperature,  
 226 and (ii) to evaluate the non-conservative source terms of potential temperature and add  
 227 these source terms to the potential temperature evolution equation during the ocean  
 228 model simulation (Tailleux, 2015).

229 However it is not possible to accurately choose the value of the isobaric heat  
 230 capacity at the sea surface that is needed when  $\theta$  is the model's temperature variable. This  
 231 issue arises because of the unresolved variations in the sea surface salinity (SSS) and SST (for  
 232 example, unresolved rain events that temporarily lower the SSS), together with the nonlinear  
 233 dependence of the isobaric specific heat on salinity and temperature. Because of such  
 234 unresolved correlations, the air-sea heat flux would be systematically mis-estimated.  
 235 Neither is it possible to accurately estimate the non-conservative source terms of  $\theta$  in the  
 236 ocean interior. This problem arises because the source terms are the product of a turbulent  
 237 flux and a mean gradient. In a mesoscale eddy-resolved ocean model (or even finer scale) it  
 238 is not clear how to find the eddy flux of  $\theta$ , as this depends on how the averaging is done in  
 239 space and time. Furthermore, when analysing the output of such an ocean model, one  
 240 would need to find a way of dealing with the contributions from source terms that are not  
 241 expressible in the form of flux convergences when, for example, estimating the meridional  
 242 heat transport.

243 We conclude that the idea that ocean models could retain potential temperature  $\theta$  as  
 244 the model's temperature variable, rather than adopt the TEOS-10 recommendation of using  
 245 Conservative Temperature  $\Theta$ , is unworkable because (1) the air-sea heat flux cannot be  
 246 accurately evaluated, (2), the non-conservative source terms that appear in the  $\theta$  evolution  
 247 equation cannot be estimated accurately, and (3) the ocean section-integrated heat fluxes

**Deleted:** This suggestion has been made, for example, by Tailleux (2015). ...

**Deleted:** Hence

**Deleted:** .

**Deleted:** one would need to deal with

**Deleted:** analyzing ocean

**Deleted:** incorporated into the ocean



255 cannot be accurately calculated. When contemplating the upgrading ocean model physics,  
256 rather than retaining the EOS-80 equation of state and treating the temperature variable as  
257 being potential temperature and having to add estimates of the non-conservative production  
258 terms to the temperature evolution equation, it is clearly much simpler and more accurate to  
259 instead adopt the TEOS-10 equation of state and to treat the model's temperature variable as  
260 Conservative Temperature, as recommended by IOC et al. (2010).

#### 261 262 *How conservative is Conservative Temperature?*

263 This question is addressed in McDougall (2003) as well as in section A.18 of the  
264 TEOS-10 Manual (IOC et al., 2010) and in Graham and McDougall (2013). The first step  
265 in addressing the non-conservation of  $\Theta$  is to find a thermophysical variable that is  
266 conserved when fluid parcels mix. McDougall (2003) and Graham and McDougall  
267 (2013) showed that when fluid parcels are brought together adiabatically and  
268 isentropically to mix at pressure  $p^m$ , it is the potential enthalpy  $h^m$  referenced to the  
269 pressure  $p^m$  of a mixing event that is conserved, apart from the dissipation of kinetic  
270 energy,  $\varepsilon$ . From this knowledge they constructed the evolution equation for  
271 Conservative Temperature (as well as for potential temperature and for entropy).

272 By contrast, Tailleux (2010) and Tailleux (2015) assumed that it was the Total  
273 Energy, being the sum of internal energy, kinetic energy and the geopotential, that is  
274 conserved when fluid parcels mix in the ocean. However, as shown by McDougall,  
275 Church and Jackett (2003), the  $-\nabla \cdot (P\mathbf{u})$  term on the right-hand side of the evolution  
276 equation for Total Energy is non-zero when integrated over the mixing region, so that  
277 Total Energy is not a conservative variable. For a variable to possess the "conservative  
278 property", it is not sufficient that the material derivative of that property is given by the  
279 divergence of a flux. Rather, what is needed is that the material derivative of a conservative  
280 variable must be equal to the divergence of a flux that is zero in the absence of mixing at that  
281 location. That is, the flux whose divergence appears on the right-hand side of the evolution  
282 equation of a conservative variable must be a diffusive flux (whether a molecular or a  
283 turbulent type of diffusive flux). This feature allows one to integrate over a region in which  
284 a mixing event is occurring and be confident that there is no flux through the bounding area

285 that lies outside of the fluid that is being mixed. This is not possible for Total Energy,  
 286 because even when integrating out to a quiescent surface that encloses an isolated patch of  
 287 turbulent mixing, the flux divergence term  $-\nabla \cdot (P\mathbf{u})$  can still be non-zero there. Note that  
 288 both contraction-on-mixing and wave processes contribute to  $-\nabla \cdot (P\mathbf{u})$ .

289 Tailleux (2010, 2015) treated this non-conservative term,  $-\nabla \cdot (P\mathbf{u})$ , as though it  
 290 were a conservative term in all their evolution equations, so that these papers actually  
 291 arrived at the correct evolution equations for  $\Theta$ ,  $\theta$  and  $\eta$  (for example, Eqn. (B.7) of  
 292 Tailleux (2010) and Eqn. (B10) of Graham and McDougall (2013) are identical).  
 293 However, these equations were written in terms of the molecular fluxes of heat and salt,  
 294 and the Tailleux (2010, 2015) papers did not find a way to use these expressions to  
 295 evaluate the non-conservation of  $\Theta$ ,  $\theta$  and  $\eta$  in a turbulently mixed ocean. This was  
 296 done in section 3 of Graham and McDougall (2013).

297 While enthalpy is conserved when mixing occurs at constant pressure, it does not  
 298 possess the “potential” property, but rather, an adiabatic and isohaline change in  
 299 pressure causes a change in enthalpy according to  $\hat{h}_p = v$ , where  $v$  is the specific  
 300 volume. This property is illustrated in Fig. 3 where it is seen that for an adiabatic and  
 301 isohaline increase of pressure of 1000dbar, the increase in enthalpy is the same as that  
 302 caused by an increase in Conservative Temperature of more than 2.4°C. If enthalpy  
 303 variations at constant pressure were a linear function of Absolute Salinity and  
 304 Conservative Temperature, the contours in Fig. 3 would be parallel equidistant straight  
 305 lines, and Conservative Temperature would be totally conservative. Since this is not the  
 306 case, this figure illustrates the (small) non-conservation of Conservative Temperature.

307 Further discussion and evaluation of the non-conservation of Conservative Temperature  
 308 can be found in McDougall (2003) and Graham and McDougall (2013).

### 310 *Seawater Salinity*

311 To a degree of approximation which is useful for many purposes, the dissolved  
 312 matter in seawater (“sea salt”) can be treated as a material of uniform composition,  
 313 whose globally averaged absolute salinity (i.e. the grams of solute per kilogram of  
 314 seawater) changes only due to the addition and removal of freshwater through rain,

315 evaporation, and river inflow. This property is because the processes that govern the  
316 addition and removal of the constituents of sea salt have extremely long time scales,  
317 relative to those that affect the pure water component of seawater. We can thus treat the  
318 total ocean salt content as approximately constant, while subject to spatially and  
319 temporally varying boundary fluxes of fresh water that give rise to salinity gradients.

320 The utility of this definition of uniform composition of sea salt lies in its  
321 conceptual simplicity, well suited to theoretical and numerical ocean modelling at time  
322 scales of up to 100s of years. However, to the demanding degree required for observing  
323 and understanding deep ocean pressure gradients, sea salt is neither uniform in  
324 composition, nor is it a conserved variable, nor can its absolute amount be measured  
325 precisely in practice. The repeatable precision of various technologies used to estimate  
326 salinity can be as small as 0.002 g/kg, but the non-ideal nature of seawater means that  
327 these estimates can be different by as much as 0.025 g/kg relative to the true Absolute  
328 Salinity in the open ocean, and as much 0.1 g/kg in coastal areas (Pawlowicz, 2015).

329 The most important interior source and sink factors governing changes in the  
330 composition of sea salt are biogeochemical processes that govern the biological uptake of  
331 dissolved nutrients, calcium, and carbon in the upper ocean, and the remineralization of  
332 these substances from sinking particles at depth. At present it is thought that changes  
333 resulting from hydrothermal vent activity, fractionation from sea ice formation, and  
334 through multi-component molecular diffusion processes are of local importance only,  
335 but little work has been done to quantify this.

336 To address this problem, TEOS-10 defines a Reference Composition of seawater,  
337 and several slightly different salinity variables that are necessary for different purposes  
338 to account for the variable composition of sea salt. The TEOS-10 Absolute Salinity,  $S_A$ ,  
339 is the absolute salinity of Reference Composition Seawater of a measured density (note  
340 that capitalization of variable names denotes a precise definition in TEOS-10). It is the  
341 salinity variable that is designed to be used to accurately calculate density using the  
342 TEOS-10 Gibbs function.

343 Prefomed Salinity,  $S_p$ , is the salinity of a seawater parcel with the effects of  
344 biogeochemical processes removed, somewhat analogous to a chlorinity-based salinity

345 estimate. It is thus a conservative tracer of seawater, suitable for modelling purposes,  
 346 but neglects the spatially variable small portion of sea salt involved in biogeochemical  
 347 processes that is required for the most accurate density estimates. Since the original  
 348 measurements of specific volume to which both EOS-80 and TEOS-10 were fitted were  
 349 made on samples of Standard Seawater with composition close to Reference  
 350 Composition, the Reference Salinity of these samples were also the same as Preformed  
 351 Salinity.

352 Ocean observational databases contain a completely different variable; Practical  
 353 Salinity. This variable, which predates TEOS-10, is essentially based on a measure of the  
 354 electrical conductance of seawater, normalized to conditions of fixed temperature and  
 355 pressure by empirical correlation equations, between the ranges of 2 and 42 PSS-78 and  
 356 scaled so that ocean salinity measurements that have been made through a variety of  
 357 technologies over the past 120 years are numerically comparable. Practical Salinity  
 358 measurement technologies involve a certified reference material called IAPSO Standard  
 359 Seawater, which for our purposes can be considered the best available artifact  
 360 representing seawater of Reference Composition.

361 Practical Salinity was not designed for numerical modelling purposes and does not  
 362 accurately represent the mass fraction of dissolved matter. We can link Practical  
 363 Salinity,  $S_p$ , to the Absolute Salinity of Reference Composition seawater (so-called  
 364 Reference Salinity,  $S_R$ ) using a fixed scale factor,  $u_{PS}$ , so that

$$365 \quad S_R = u_{PS} S_p \quad \text{where} \quad u_{PS} \equiv (35.165\,04/35) \text{ g kg}^{-1}. \quad (3)$$

366 Conversions to and between the other “salinity” definitions, however, involve  
 367 knowledge about spatial and temporal variations in seawater composition. Fortunately,  
 368 the largest component of these changes occurs in a set of constituents involved in  
 369 biogeochemical processes, whose co-variation is known to be strongly correlated. Thus  
 370 the Absolute Salinity of real seawater can be determined globally to useful accuracy  
 371 from the Reference Salinity by the addition of a single parameter, the so-called Absolute  
 372 Salinity Anomaly,  $\delta S_A$ ,

$$373 \quad S_A = S_R + \delta S_A, \quad (4)$$

374 which has been tabulated in a global atlas for the current ocean (McDougall et al., 2012),  
 375 and is estimated in coastal areas by considering the effects of river salts (Pawlowicz,  
 376 2015). It can also be determined from measurements of either density or of carbon and  
 377 nutrients (IOC et al., 2010, [Ji et al., 2021](#)). For purposes of numerical ocean modelling,  
 378 the Absolute Salinity Anomaly could in theory be obtained by separately tracking the  
 379 carbon cycle and nutrients, and applying known correction factors, but we are not aware  
 380 of any attempts to do so.

381 Chemical modelling (Pawlowicz (2010), Wright et al. (2011), Pawlowicz et al.  
 382 (2012)) suggests the approximate relation

$$383 \quad S_A - S_* \approx 1.35 \delta S_A \equiv 1.35(S_A - S_R), \quad (5)$$

384 and these relationships are schematically illustrated in Fig. 4. The magnitude of the  
 385 Absolute Salinity Anomaly is around  $-0.005$  to  $+0.025$  g/kg in the open ocean, relative to a  
 386 mean Absolute Salinity of about 35 g/kg. The correction it implies may be important  
 387 when initializing models, or comparing them with observations, but its major effect is  
 388 likely in producing biases in calculated isobaric density gradients.

389

390

### 391 *Seawater density*

392 The density of seawater is the most important thermodynamic property affecting  
 393 oceanic motions, since its spatial changes (along with changes to the sea-surface height)  
 394 give rise to pressure gradients which are the primary driving force for currents within  
 395 the ocean interior through the hydrostatic relation. The “traditional” equation of state is  
 396 known as EOS-80 (UNESCO, 1981), and is standardized as a function of Practical  
 397 Salinity and in-situ temperature,  $\rho = \rho(S_p, t, p)$  which has 41 numerical terms. An  
 398 additional equation (the adiabatic lapse rate) is required for conversion of temperature  
 399 to potential temperature. However, for ocean models, the EOS-80 equation of state is  
 400 usually taken to be the 41-term expression written in terms of potential temperature,  
 401  $\rho = \tilde{\rho}(S_p, \theta, p)$ , of Jackett and McDougall (1995), where the over-twiddle indicates that  
 402 this rational function fit was made with Practical Salinity  $S_p$  and potential temperature  
 403  $\theta$  as the input salinity and temperature variables.

404 The current standard for describing the thermodynamic properties of seawater,  
 405 known as TEOS-10, provides an equation of state,  $v = 1/\rho = v(S_A, t, p)$ , in the form of a  
 406 function which involves 72 coefficients (IOC et al., 2010) and is an analytical pressure  
 407 derivative of the TEOS-10 Gibbs function. However, for ocean models using TEOS-10  
 408 the equation of state used is one of those in Roquet et al. (2015); the 55-term equation of  
 409 state,  $\rho = \hat{\rho}(S_A, \Theta, z)$ , used by Boussinesq models and the 75-term polynomial for specific  
 410 volume,  $v = \hat{v}(S_A, \Theta, p)$ , used by non-Boussinesq ocean models.

411 In this paper we will not concentrate on the distinction between Boussinesq and  
 412 non-Boussinesq ocean models, and henceforth we will take the third input to the  
 413 equation of state to be pressure, even though for a Boussinesq model it is in fact a scaled  
 414 version of depth as per the energetic arguments of Young (2010). By the same token, we  
 415 will cast the discussion in terms of the *in situ* density, even though the non-Boussinesq  
 416 models have as their equation of state a polynomial for the specific volume,  $v = 1/\rho$ .

417 For seawater of Reference Composition, both the TEOS-10 and EOS-80 fits  
 418  $\rho = \hat{\rho}(S_A, \Theta, p)$  and  $\rho = \tilde{\rho}(S_p, \theta, p)$  are almost equally accurate (see section A.5 of IOC et  
 419 al. (2010) and note the comparison between Figures A.5.1 and A.5.2 therein). That is, if  
 420 we set  $\delta S_A = 0$  and use Eqn. (3) to relate Practical and Reference Salinities (which in this  
 421 case are the same as Preformed Salinities), the numerical density values of in situ density  
 422 calculated using EOS-80 are not significantly different to those using TEOS-10 [in the](#)  
 423 [open ocean \[the differences are significant for brackish waters\]](#).

424 This being the case, we can see from sections A.5 and A.20 of the TEOS-10  
 425 Manual (IOC et al. (2010)) that 58% of the data deeper than 1000 dbar in the World  
 426 Ocean would have the thermal wind misestimated by ~2.7% due to ignoring the  
 427 difference between Absolute and Reference Salinities. No ocean model has addressed  
 428 this deficiency to date, but McCarthy et al. (2015) studied the influence of using Absolute  
 429 Salinity versus Reference Salinity in calculating the overturning circulation in the North  
 430 Atlantic. They found that the overturning streamfunction changed by 0.7Sv at a depth  
 431 of 2700m, relative to a mean value at this depth of about 7 Sv, i.e., a 10% effect. Because  
 432 we argue that the salinity variable in ocean models is best interpreted as being  
 433 Preformed Salinity,  $S_*$ , the neglect of the distinction between Preformed and Absolute

434 Salinities in ocean models means that they misestimate the overturning streamfunction  
 435 by 1.35 (see Figure 4) times 0.7Sv, namely ~1Sv, i.e., a 13.5% effect.

436

#### 437 *Air-sea heat fluxes*

438 Sensible, latent and long-wave radiative fluxes are affected by near-surface  
 439 turbulence and are usually calculated using bulk formulae involving air and sea  
 440 surface water temperatures (the air and sea *in situ* temperatures), as well as other  
 441 parameters (e.g., the latent heat involves the isobaric evaporation enthalpy, commonly  
 442 called the latent heat of evaporation, which is actually a weak function of temperature  
 443 and salinity; see Eqn. 6.28 of Feistel et al. (2010) and Eqn. (3.39.7) of IOC et al. (2010)).  
 444 The total air-sea heat flux,  $Q$ , is then translated into a water temperature change by  
 445 dividing by a heat capacity  $c_p^0$ , which has always been taken to be constant in  
 446 numerical models (Griffies et al., 2016). Although this method is appropriate for  
 447 Conservative Temperature, CT, (assuming that the TEOS-10 value is used for  $c_p^0$ ), it is  
 448 not appropriate when potential temperature is being considered. The flux of potential  
 449 temperature into the surface of the ocean should be  $Q$  divided by  $c_p(S_s, \theta, 0)$ . The use  
 450 of a constant specific heat capacity, in association with the interpretation of the  
 451 ocean's temperature variable as being potential temperature, means that the ocean has  
 452 received a different amount of heat than the atmosphere actually delivers to the ocean,  
 453 and this issue will be explored in section 3.

454 When precipitation ( $P$ ) occurs at the sea surface, this addition of freshwater  
 455 brings with it the associated potential enthalpy  $h(S_A=0, t, 0\text{dbar})$  per unit mass of  
 456 freshwater, where  $t$  is the *in situ* temperature of the rain drops as they arrive at the sea  
 457 surface. The temperature at which rain enters the ocean is not yet treated consistently in  
 458 coupled models, and section K1.6 of Griffies et al. (2016) suggests that this effect could  
 459 be equivalent to an area-averaged extra air-sea heat flux of between  $-150 \text{ mW m}^{-2}$   
 460 and  $-300 \text{ mW m}^{-2}$ , representing a heat loss for the ocean.

461

462

463

## 464 *Numerical ocean models*

465 In deciding how to numerically model the ocean, an explicit choice must be made  
 466 about the equation of state, and one would think that this choice would have  
 467 implications about the precise meaning of the temperature and salinity variables in the  
 468 model, which we will call  $T_{\text{model}}$  and  $S_{\text{model}}$  respectively. We can divide ocean models  
 469 into two general classes, EOS-80 models, and TEOS-10 models:

470

### 471 EOS-80 models

472 One class of CMIP ocean model is based around EOS-80, and these models have the  
 473 following characteristics:

- 474 1. The model's equation of state,  $\rho = \bar{\rho}(S_p, \theta, p)$ , expects to have Practical Salinity  
 475 and potential temperature as the salinity and temperature input parameters.
- 476 2.  $T_{\text{model}}$  is advected and diffused in the ocean interior in a conservative manner, i.e.,  
 477 its evolution at a point in space is determined by the convergence of advective  
 478 fluxes plus parameterized sub-grid scale diffusive and skew diffusive fluxes.
- 479 3.  $S_{\text{model}}$  is advected and diffused in the ocean interior in a conservative manner as  
 480 for  $T_{\text{model}}$ .
- 481 4. The air-sea heat flux is delivered to/from the ocean using a constant isobaric  
 482 specific heat,  $c_p^0$ , to convert the air-sea heat flux into a surface flux of  $T_{\text{model}}$ . [An  
 483 EOS-80 based model's value of  $c_p^0$  is generally only slightly different to the  
 484 TEOS-10 value.]
- 485 5.  $T_{\text{model}}$  is initialized from an atlas of values of potential temperature, and  $S_{\text{model}}$  is  
 486 initialized with values of Practical Salinity.

487 At first glance, it seems reasonable to assume that  $T_{\text{model}}$  is potential temperature, and  
 488  $S_{\text{model}}$  is Practical Salinity. However, these assumptions imply that theoretical errors  
 489 arising from items 2 and 3 and 4 are ignored (since neither potential temperature nor  
 490 Practical Salinity are conservative variables). In this paper we show that these  
 491 interpretations of the model's temperature and salinity variables are not as accurate as  
 492 our proposed alternative interpretations.

493



494 TEOS-10 models

495 Other ocean models have begun to implement TEOS-10 features. These models  
496 generally have the following characteristics.

- 497 1. The model's equation of state,  $\rho = \hat{\rho}(S_A, \Theta, p)$ , expects to have Absolute Salinity  
498 and Conservative Temperature as its salinity and temperature input parameters.
- 499 2.  $T_{\text{model}}$  is advected and diffused in the ocean interior in a conservative manner.
- 500 3.  $S_{\text{model}}$  is advected and diffused in the ocean interior in a conservative manner.
- 501 4. At each time step of the model, the value of potential temperature at the sea  
502 surface (i.e. SST) is calculated from the  $T_{\text{model}}$  (which is assumed to be  
503 Conservative Temperature) and this value of SST is used to interact with the  
504 atmosphere via bulk flux formulae.
- 505 5. The air-sea heat flux is delivered to/from the ocean using the TEOS-10 constant  
506 isobaric specific heat,  $c_p^0$ , to convert the air-sea heat flux into a surface flux of  
507  $T_{\text{model}}$ .
- 508 6.  $T_{\text{model}}$  is initialized from an atlas of values of Conservative Temperature, and  
509  $S_{\text{model}}$  is initialized with values of one of Absolute Salinity, Reference Salinity or  
510 Preformed Salinity.

511 Implicitly, it has then been assumed that  $T_{\text{model}}$  is a Conservative Temperature, and  $S_{\text{model}}$   
512 is Absolute Salinity.

513 There is one CMIP6 ocean model that we are aware of, ACCESS-CM2 (Australian  
514 Community Climate and Earth System Simulator, Bi et al. 2013), whose equation of state  
515 is written in terms of Conservative Temperature, but the salinity argument in the  
516 equation of state is Practical Salinity. The salinity in this model is initialized with atlas  
517 values of Practical Salinity.

518 From the above it is clear that there are small but significant theoretical  
519 incompatibilities between different models, and between models and the observed  
520 ocean. These issues become apparent when dealing with the technicalities of  
521 intercomparisons, and various choices must be made. We now consider the implications  
522 of these different choices and provide recommendations for best practices.

523

524 **3. The Interpretation of salinity in ocean models**

525 Note that the samples whose measured specific volumes were incorporated into  
 526 both the EOS-80 and TEOS-10 equations of state were of Standard Seawater whose  
 527 composition is close to Reference Composition. Consequently, the EOS-80 and TEOS-10  
 528 equations of state were constructed with Prefomed Salinity,  $S_*$  (or, in the case of EOS-  
 529 80 models,  $S_*/u_{\text{ps}}$ ), as their salinity arguments, not Reference Salinity. These same  
 530 algorithms give accurate values of specific volume for seawater samples that are not of  
 531 Reference Composition so long as the salinity argument is Absolute Salinity (as opposed  
 532 to Reference Salinity or Prefomed Salinity).

533 For an ocean model that has no non-conservative interior source terms affecting  
 534 the evolution of its salinity variable, and that is initialized at the sea surface with  
 535 Prefomed Salinity, the only interpretation for the model's salinity variable is Prefomed  
 536 Salinity, and the use of the TEOS-10 equation of state will then yield the correct specific  
 537 volume. Furthermore, whether the model is initialized with values of Absolute Salinity,  
 538 Reference Salinity or Prefomed Salinity, these initial salinity values are nearly identical  
 539 in the upper ocean, and any differences between the three initial conditions in the  
 540 deeper ocean would be largely diffused away within the long spin-up period. That is, in  
 541 the absence of the non-conservative biogeochemical source terms that would be needed  
 542 to model Absolute Salinity and to force it away from being conservative (or the smaller  
 543 source terms that would be needed to maintain Reference Salinity), the model's salinity  
 544 variable will drift towards being Prefomed Salinity. Hence, we conclude that, after the  
 545 long spin-up phase, the salinity variable of a TEOS-10 based ocean model is accurately  
 546 interpreted as being Prefomed Salinity  $S_*$ , irrespective of whether the model was  
 547 initialized with values of Absolute Salinity, Reference Salinity or Prefomed Salinity.

548 Likewise, the prognostic salinity variable after a long spin-up period of an EOS-  
 549 80 based model is most accurately interpreted as being Prefomed Salinity divided by  
 550  $u_{\text{ps}} \equiv (35.165\ 04/35)\ \text{g kg}^{-1}$ ,  $S_*/u_{\text{ps}}$ .

551 We clearly need more estimates of the magnitude of the dynamic effects of the  
 552 variable seawater composition, but for now we might take a change in 1 Sv in the  
 553 meridional transport of deep water masses in each ocean basin (based on the Atlantic

554 work of McCarthy et al., 2015) as an indication of the magnitude of the effect of  
555 neglecting the effects of biogeochemistry on salinity. At this stage of model  
556 development, since all models are equally deficient in their thermophysical treatment of  
557 salinity, at least this aspect does not present a problem as far as making comparisons  
558 between CMIP models.

559

#### 560 **4. Model Heat Flux Calculations**

561 From the details described above, both types of numerical ocean models suffer from  
562 some internal contradictions with thermodynamical best practice. For example, for the  
563 EOS-80 based models, if  $T_{\text{model}}$  is assumed to be potential temperature, the use of EOS-80  
564 is correct for density calculations but the use of conservative equations for  $T_{\text{model}}$  ignores  
565 the non-conservative production of potential temperature. The use of a constant heat  
566 capacity is also in error if  $T_{\text{model}}$  is interpreted as potential temperature. Conservative  
567 equations are, however, appropriate for Conservative Temperature. In addition, if  $S_{\text{model}}$   
568 is assumed to be either Practical Salinity or Absolute Salinity, then the use of  
569 conservative equations ignores the changes in salinity that arise from biogeochemical  
570 processes.

571 One use for these models is to calculate heat budgets and heat fluxes – both at the  
572 surface and between latitudinal bands, and inherent to CMIP is the idea that these  
573 different models should be intercompared. The question of how this intercomparison  
574 should be done, however, was not clearly addressed in Griffies et al. (2016). Here we  
575 begin the discussion by considering two different options for interpreting  $T_{\text{model}}$  in EOS-  
576 80 ocean models.

577

##### 578 **4.1 Option 1: interpreting the EOS-80 model's temperature as being potential** 579 **temperature**

580 Under this option the model's temperature variable  $T_{\text{model}}$  is treated as being potential  
581 temperature  $\theta$ ; this is the prevailing interpretation to date. With this interpretation of  
582  $T_{\text{model}}$  one wonders whether Conservative Temperature  $\Theta$  should be calculated from the  
583 model's (assumed) potential temperature before calculating (i) the global Ocean Heat

584 Content as the volume integral of  $\rho c_p^0 \Theta$ , and (ii) the advective meridional heat transport  
585 as the area integral of  $\rho c_p^0 \Theta v$  at constant latitude, where  $v$  is the northward velocity.  
586 This question was not clearly addressed in Griffies et al. (2016), and here we emphasize  
587 one of the main conclusions of the present paper, namely that ocean heat content and  
588 meridional heat transports should be calculated using the model's prognostic  
589 temperature variable. Any subsequent conversion from one temperature variable to  
590 another (such as potential to Conservative) in order to calculate heat content and heat  
591 transport is incorrect and confusing, and should not be attempted.

592

#### 593 *4.1.1 Issues with the potential temperature interpretation*

594 There are several thermodynamic inconsistencies that arise from option 1. First,  
595 the ocean model has assumed in its spin-up phase (for perhaps a millennium) that  $T_{\text{model}}$   
596 is conservative, so during the whole spin-up phase and beyond, the contribution of the  
597 known non-conservative interior source terms of potential temperature have been  
598 absent, and hence the model's temperature variable has not responded to these absent  
599 source terms and so this temperature field cannot be potential temperature. Also, since  
600 the temperature field of the model is not potential temperature (because of these absent  
601 source terms) the velocity field of the model will also not be forced correctly due to  
602 errors in the density field which in turn affect the pressure force.

603 The second inconsistent aspect of option 1 is that the air-sea flux of heat is  
604 ingested into the ocean model, both during the spin-up stage and during the subsequent  
605 transient response phase, as though the model's temperature variable is proportional to  
606 potential enthalpy. For example, consider some time during the year at a particular  
607 location where the sea surface is fresh (a river outflow, or melted ice). During this time,  
608 any heat that the atmosphere loses or gains should have affected the potential  
609 temperature of the upper layers of the ocean using a specific heat that is 6% larger than  
610  $c_p^0$  (see Figure 1). So, if the ocean model's temperature variable is interpreted as being  
611 potential temperature, a 6% error is made in the heat flux that is exchanged with the  
612 atmosphere during these periods/locations. That is, the changes in the ocean model's  
613 (assumed) potential temperature caused by the air-sea heat flux will be exaggerated

614 where and when the sea surface salinity is fresh. This 6% flux error is not corrected by  
 615 subsequently calculating Conservative Temperature from potential temperature; for  
 616 example, these temperatures are the same at low temperature and salinity (see Figure 2),  
 617 and yet at low values of salinity, the specific heat is 6% larger than  $c_p^0$ .

618 This second inconsistent aspect of option 1 can be restated as follows. The  
 619 adoption of potential temperature as the model's temperature variable means that there  
 620 is a discontinuity in the heat flux of the coupled air-sea system right at the sea surface;  
 621 for every Joule of heat (i.e. potential enthalpy) that the atmosphere gives to the ocean,  
 622 under this Option 1 interpretation, up to 6% too much heat arrives in the ocean over  
 623 relatively fresh waters. In this way, the adoption of potential temperature as the model  
 624 temperature variable ensures that the coupled ocean atmosphere system will not  
 625 conserve heat. Rather, there appear to be non-conservative sources and sinks of heat  
 626 right at the sea surface where heat is unphysically manufactured or destroyed.

627 The third inconsistent aspect is a direct consequence of the second; namely that if  
 628 one is tempted to post-calculate Conservative Temperature  $\Theta$  from the model's  
 629 (assumed) values of potential temperature, the rate of change of the calculated ocean  
 630 heat content as the volume integral of  $\rho c_p^0 \Theta$  would no longer be accurately related to the  
 631 heat that the atmosphere exchanged with the ocean. Neither would the area integral  
 632 between latitude bands of the air-sea heat flux be exactly equal to the difference between  
 633 the calculated oceanic meridional heat transports that cross those latitudes. Rather,  
 634 during the running of the model the heat that was lost from the atmosphere actually  
 635 shows up in the ocean as the volume integral of the model's prognostic temperature  
 636 variable. Thus we agree with Appendix D3.3 of Griffies et al. (2016) and strongly  
 637 recommend that Conservative Temperature is not calculated *a posteriori* in order to  
 638 evaluate heat content and heat fluxes in these EOS-80 based models.

639

#### 640 4.1.2 Quantifying the air-sea flux imbalance

641 Here we quantify the air-sea flux errors involved with assuming that  $T_{\text{model}}$  of  
 642 EOS-80 models is potential temperature. These EOS-80 based models calculate the air-  
 643 sea flux of their model's temperature as the air-sea heat flux,  $Q$ , divided by  $c_p^0$ .

644 However, since the isobaric specific heat capacity of seawater at 0 dbar is  $c_p(S_*,\theta,0)$ , the  
 645 flux of potential temperature into the surface of the ocean should be  $Q$  divided by  
 646  $c_p(S_*,\theta,0)$ . So, if the model's temperature variable is interpreted as being potential  
 647 temperature, the EOS-80 model has a flux of potential temperature entering the ocean  
 648 that is too large by the difference between these fluxes, namely by  $Q/c_p^0$  minus  
 649  $Q/c_p(S_*,\theta,0)$ . This means that the ocean has received a different amount of heat than the  
 650 atmosphere actually delivers to the ocean, with the difference,  $\Delta Q$ , being  $c_p(S_*,\theta,0)$   
 651 times the difference in the surface fluxes of potential temperature, namely (for the last  
 652 part of this equation, see Eqn. (A.12.3a) of IOC et al., 2010)

$$653 \quad \Delta Q = Q \left( \frac{c_p(S_*,\theta,0)}{c_p^0} - 1 \right) = Q(\tilde{\Theta}_\theta - 1). \quad (6)$$

654 We plot this quantity from the pre-industrial control run of ACCESS-CM2 in  
 655 Figure 5c and show it as a cell area-weighted histogram in Figure 5e (note that while  
 656 these plots apply to EOS-80 based ocean models, to generate these plots we have  
 657 actually used data from ACCESS-CM2 which is a mostly TEOS-10 compliant model).  
 658 The calculation takes into account the penetration of shortwave radiation into the ocean  
 659 but is performed using monthly averages of the thermodynamics quantities. The  
 660 temperatures and salinities at which the radiative flux divergences occur are taken into  
 661 account in this calculation. However, the result is little changed if the sea surface  
 662 temperatures and salinities are used with the radiative flux divergence assumed to take  
 663 place at the sea surface. Results from similar calculations performed using monthly and  
 664 daily averaged quantities in ACCESS-OM2 (Kiss et al. 2020) ocean-only model  
 665 simulations were similar, suggesting that correlations between sub-monthly variations  
 666 are not significant in such a relatively coarse-resolution model.

667  $\Delta Q$  has an area-weighted mean value of  $16 \text{ mW m}^{-2}$  and we know that this  
 668 represents the net surface flux of potential temperature required to balance the volume  
 669 integrated non-conservation of potential temperature in the ocean's interior (Tailleux  
 670 (2015)). To put this value in context,  $16 \text{ mW m}^{-2}$  corresponds to 5% of the observed trend  
 671 of  $300 \text{ mW m}^{-2}$  in the global ocean heat content from 1955-2017 (Zanna et al. 2019). In  
 672 addition to this mean value of  $\Delta Q$ , we see from Figure 5c that there are regions such as

673 the equatorial Pacific and the western north Pacific where  $\Delta Q$  is as large as the area-  
674 averaged heat flux,  $300 \text{ mWm}^{-2}$ , that the ocean has received since 1955. These local  
675 anomalies of air-sea flux, if they existed, would drive local variations in temperature.  
676 However, these  $\Delta Q$  values do not represent real heat fluxes. Rather they represent the  
677 error in the air-sea heat flux that we make if we insist that the temperature variable in an  
678 EOS-80 based ocean model is potential temperature, with the ocean receiving a surface  
679 heat flux that is larger by  $\Delta Q$  than the atmosphere delivers to the ocean. Figure 6 shows  
680 the zonal integration of  $\Delta Q$ , in units of W per degree of latitude.

681 Figure 5e shows that, with  $T_{\text{model}}$  being interpreted as potential temperature, 5%  
682 of the surface area of the ocean needs a surface heat flux that is more than  $135 \text{ mWm}^{-2}$   
683 different to what the atmosphere gives to/from the ocean. This regional variation of  $\Delta Q$   
684 of approximately  $\pm 100 \text{ mWm}^{-2}$  is consistent with the regional variations in the air-sea  
685 flux of potential temperature found by Graham and McDougall (2013) that is needed to  
686 balance the depth-integrated non-conservation of potential temperature as a function of  
687 latitude and longitude. This damage that is done to the air-sea heat flux at a given  
688 horizontal location by the interpretation that the temperature variable of an EOS-80 ocean  
689 model is potential temperature is not small in comparison to the globally averaged rate that  
690 our planet is being anthropogenically warmed. That is, in regions that are comparable in  
691 size to an ocean basin (see Figure 5(c)), a heat budget analysis using EOS-80 and potential  
692 temperature would find a false trend as large as the globally averaged rate that our planet is  
693 warming.

694 Figures 5d,f show that much of this spread is due to the variation of the isobaric  
695 specific heat capacity on salinity, with the remainder due to the variation of this heat  
696 capacity with temperature. We note that if this analysis were performed with a model  
697 that resolved individual rain showers and the associated freshwater lenses on the ocean  
698 surface, then these episodes of very fresh water at the sea surface would be expected to  
699 increase the calculated values of  $\Delta Q$ . Interestingly, by way of contrast, it is the variation  
700 of the isobaric heat capacity with temperature that dominates (by a factor of four) the  
701 contribution of this heat capacity variation to the *area-mean* of  $\Delta Q$  (with the contribution

702 of salinity,  $\Delta Q_s$ , in Figure. 5d, leading to an area mean of  $4 \text{ mW m}^{-2}$ ), as originally found  
703 by Tailleux (2015).

704 While a heat flux error of  $\pm 100 \text{ mW m}^{-2}$  is not large, it also not trivially small, and  
705 it seems advisable to respect these fundamental thermodynamic aspects of the coupled  
706 Earth system. We will see that this  $\pm 100 \text{ mW m}^{-2}$  issue is simply avoided by realizing  
707 that the temperature variable in these EOS-80 models is not potential temperature.

708 In Appendix A we enquire whether the way that EOS-80 models treat their fluid  
709 might be made to be thermodynamically correct for a fluid other than seawater. We find  
710 that it is possible to construct such a thermodynamic definition of a fluid with the aim  
711 that its treatment in EOS-80 models is consistent with the laws of thermodynamics. This  
712 fluid has the same specific volume as seawater for given values of salinity, potential  
713 temperature and pressure, but it has different expressions for both enthalpy and  
714 entropy. This fluid also has a different adiabatic lapse rate and therefore a different  
715 relationship between *in situ* and potential temperatures. However, this exercise in  
716 thermodynamic abstraction does not alter the fact that, as a model of the real ocean, and  
717 with the temperature variable being interpreted as being potential temperature, the  
718 EOS-80 models have  $\Delta Q$  more heat arriving in the ocean than leaves the atmosphere.

719 Since CMIP6 is centrally concerned with how the planet warms, it is advisable to  
720 adopt a framework where heat fluxes and their consequences are respected. That is, we  
721 regard it as imperative to avoid non-conservative sources of heat at the sea surface. It is  
722 the insistence that the temperature variable in EOS-80 based models is potential  
723 temperature that implies that the ocean receives a heat flux from the atmosphere that is  
724 larger by  $\Delta Q$  than what the atmosphere actually exchanges with the ocean. Since there  
725 are some areas of the ocean surface where  $\Delta Q$  is as large as the mean rate of global  
726 warming, Option 1 is not supportable. This situation motivates Option 2 where we  
727 change the interpretation of the model's temperature variable from being potential  
728 temperature to Conservative Temperature even when using EOS-80.

729

#### 730 **4.2 Option 2: interpreting the EOS-80 model's temperature as being Conservative**

##### 731 **Temperature**



732 Under this option the ocean model's temperature variable is taken to be Conservative  
 733 Temperature  $\Theta$ . The air-sea flux of potential enthalpy is then correctly ingested into the  
 734 ocean model using the fixed specific heat  $c_p^0$ , and the mixing processes in the model  
 735 correctly conserve Conservative Temperature. Hence the second, fourth and fifth items  
 736 listed in section 2 are handled correctly, except for the following caveat. In the coupled  
 737 model, the bulk formulae that set the air-sea heat flux at each time step use the  
 738 uppermost model temperature as the sea surface temperature as input. So with the  
 739 Option 2 interpretation of the model's temperature variable as being Conservative  
 740 Temperature, these bulk formulae are not being fed the SST (which at the sea surface is  
 741 equal to the potential temperature  $\theta$ ). The difference between these temperatures is  
 742  $\Theta - \theta$ , which is the negative of what we plot in Figure 2. This is a caveat with this  
 743 Option 2 interpretation, namely that the bulk formula that the model uses to determine  
 744 the air-sea flux at each time step is a little different to what was intended when the  
 745 parameters of the bulk formulae were chosen. This is a caveat regarding what was  
 746 intended by the coupled modeler, rather than what the coupled model experienced.  
 747 That is, with this Option 2 interpretation, the air-sea heat flux, while being a little bit  
 748 different than what might have been intended, does arrive in the ocean properly; there is  
 749 no non-conservative production or destruction of heat at the air-sea boundary as there is  
 750 in Option 1.

751       Regarding the remaining two items involving temperature listed in section 2, we  
 752 can dismiss the fifth item, since any small difference in the initial values, set at the  
 753 beginning of the lengthy spin-up period, between potential temperature and  
 754 Conservative Temperature will be irrelevant after the long spin-up integration.

755       This then leaves the first point, namely that the model used the equation of state  
 756 that expects potential temperature as its temperature input,  $\tilde{\rho}(S_*/u_{ps}, \theta, p)$ , but under  
 757 this Option 2 we are interpreting the model's temperature variable as being  
 758 Conservative Temperature. In the remainder of this section we address the magnitude  
 759 of this effect, namely, the use of  $\tilde{\rho}(S_*/u_{ps}, \Theta, p)$  versus the correct density  $\tilde{\rho}(S_*/u_{ps}, \theta, p)$   
 760 which is almost the same as  $\hat{\rho}(S_*, \Theta, p)$ . Note, as discussed in section 3 above, the  
 761 salinity argument of the TEOS-10 equation of state is taken to be  $S_*$  while that of the

762 EOS-80 equation of state is taken to be  $S_*/u_{ps}$ . These salinity variables are simply  
763 proportional to each other, and they have the same influence in both equations of state.

764 Under this Option 2 we are interpreting the model's temperature variable as  
765 being Conservative Temperature, and so the density value that the model calculates  
766 from its equation of state is deemed to be  $\tilde{\rho}(S_*/u_{ps}, \Theta, p)$  whereas the density should be  
767 evaluated as  $\hat{\rho}(S_*, \Theta, p)$  where we remind ourselves that the hat over the *in situ* density  
768 function indicates that this is the TEOS-10 equation of state, written with Conservative  
769 Temperature as its temperature input. To be clear, under EOS-80 and under TEOS-10  
770 the *in situ* density of seawater of Reference Composition has been expressed by two  
771 different expressions,

$$772 \quad \rho = \tilde{\rho}(S_*/u_{ps}, \theta, p) = \hat{\rho}(S_*, \Theta, p), \quad (7)$$

773 both of which are very good fits to the *in situ* density (hence the equals signs); the  
774 increased accuracy of the TEOS-10 equation for density was mostly due to the  
775 refinement of the salinity variable, and the increase in the accuracy of TEOS-10 versus  
776 EOS-80 for Standard Seawater (Millero et al., 2008) was minor by comparison except for  
777 brackish seawater.

778 We need to ask what error will arise from calculating *in situ* density in the model  
779 as  $\tilde{\rho}(S_*/u_{ps}, \Theta, p)$  instead of as the correct TEOS-10 version of *in situ* density,  $\hat{\rho}(S_*, \Theta, p)$ ?  
780 The effect of this difference on calculations of the buoyancy frequency and even the  
781 neutral tangent plane is likely small, so we concentrate on the effect of this difference on  
782 the isobaric gradient of *in situ* density (the thermal wind).

783 Given that under this Option 2 the model's temperature variable is being  
784 interpreted as Conservative Temperature,  $\Theta$ , the model-calculated isobaric gradient of  
785 *in situ* density is

$$786 \quad \tilde{\rho}_{S_*} \nabla_p S_* + \tilde{\rho}_{\Theta} \nabla_p \Theta, \quad (8)$$

787 whereas the correct isobaric gradient of *in situ* density is actually

$$788 \quad \hat{\rho}_{S_*} \nabla_p S_* + \hat{\rho}_{\Theta} \nabla_p \Theta. \quad (9)$$

789 Notice that here and henceforth we drop the scaling factor  $u_{ps}$  from the gradient  
790 expressions such as Eqn. (8). In any case, this scaling factor cancels from the expression,  
791 but we simply drop it for ease of looking at the equations; we can imagine that the EOS-

792 80 equation of state is written in terms of  $S_*$  (which would simply require that a first  
793 line is added to the computer code which divides the salinity variable by  $u_{ps}$ ).

794 The model's error in evaluating the isobaric gradient of *in situ* density is then the  
795 difference between the two equations above, namely

$$796 \quad \text{error in } \nabla_p \rho = (\tilde{\rho}_{S_*} - \hat{\rho}_{S_*}) \nabla_p S_* + (\tilde{\rho}_\theta - \hat{\rho}_\theta) \nabla_p \Theta. \quad (10)$$

797 The relative error here in the temperature derivative of the equations of state can be  
798 written approximately as

$$799 \quad (\tilde{\rho}_\theta - \hat{\rho}_\theta) / \hat{\rho}_\theta = \tilde{\alpha}^\theta / \hat{\alpha}^\theta - 1, \quad (11)$$

800 which is the difference from unity of the ratio of the thermal expansion coefficient with  
801 respect to potential temperature to that with respect to Conservative Temperature. This  
802 ratio,  $\tilde{\alpha}^\theta / \hat{\alpha}^\theta$ , can be shown to be equal to  $c_p(S_*, \theta, 0) / c_p^0$  and we know (from Figure 1)  
803 that this varies by 6% in the ocean. This ratio is plotted in Figure 7(a). In regions of the  
804 ocean that are very fresh, a relative error in the contribution of the isobaric temperature  
805 gradient to the thermal wind will be as large as 6% while in most of the ocean this  
806 relative error will be less than 0.5%.

807 Now we turn our attention to the relative error in the salinity derivative of the  
808 equation of state, which, from Eqn. (10) can be written approximately as

$$809 \quad (\tilde{\rho}_{S_*} - \hat{\rho}_{S_*}) / \hat{\rho}_{S_*} = \tilde{\beta}^\theta / \hat{\beta}^\theta - 1, \quad (12)$$

810 and the ratio,  $\tilde{\beta}^\theta / \hat{\beta}^\theta$ , has been plotted (at  $p = 0$ bar) in Figure 7(b). This figure shows  
811 that the relative error in the salinity derivative,  $(\tilde{\rho}_{S_*} - \hat{\rho}_{S_*}) / \hat{\rho}_{S_*}$ , is an increasing  
812 (approximately quadratic) function of temperature, being approximately zero at 0°C, 1%  
813 error at 20°C and 2% error at 30°C. An alternative derivation of these implications of  
814 Eqn. (10) is given in Appendix B.

815 We conclude that under Option 2, where the temperature variable of an EOS-80  
816 based model (whose polynomial equation of state expects to have potential temperature  
817 as its input temperature) is interpreted as being Conservative Temperature, there are  
818 persistent errors in the contribution of the isobaric salinity gradient to the isobaric  
819 density gradient that are approximately proportional to temperature squared, with the  
820 error being approximately 1% at a temperature of 20°C (mostly due to the salinity

821 derivative of *in situ* density at constant potential temperature being 1% different to the  
 822 corresponding salinity derivative at constant Conservative Temperature). Larger  
 823 fractional errors in the contribution of the isobaric temperature gradient to the thermal  
 824 wind equation do occur (of up to 6%) but these are restricted to the rather small volume  
 825 of the ocean that is quite fresh.

826 In Figure 8 we have evaluated how much the meridional isobaric density  
 827 gradient changes in the upper 1000 dbar of the World Ocean when the temperature  
 828 argument in the expression for density is switched from  $\theta$  to  $\Theta$ . As explained above,  
 829 this switch is almost equivalent to the density difference between calling the EOS-80 and  
 830 the TEOS-10 equations of state, using the same numeric inputs for each. We find that  
 831 19% of this data has the isobaric density gradient changed by more than 1% when  
 832 switching from  $\theta$  to  $\Theta$ . The median value of the percentage error is 0.22%; that is, 50%  
 833 of the data shallower than 1000 dbar has the isobaric density gradient changed by more  
 834 than 0.22% when switching from using EOS-80 to TEOS-10, with the same numerical  
 835 temperature input, which we are interpreting as being  $\Theta$ .

836 Figure 8 should not be interpreted as being the extra error involved with taking  
 837  $T_{\text{model}}$  to be Conservative Temperature in EOS-80 ocean models, because, due to the lack  
 838 of interior non-conservative source terms, the interpretation of  $T_{\text{model}}$  as being potential  
 839 temperature is already incorrect by an amount that scales as  $\Theta$  minus  $\theta$ . Rather, Figure  
 840 8 illustrates the error in an EOS-80 model due to the use of an equation of state that is  
 841 not appropriate to the way that its temperature variable is treated in the model.

842  
 843  
 844

#### 845 4.3 Evaluating the options for EOS-80 models

846 Under option 1 where  $T_{\text{model}}$  is interpreted as potential temperature, there is a  
 847 non-conservation of heat at the sea surface, with the ocean seeing one heat flux, and the  
 848 atmosphere immediately above it seeing another, with 5% of the differences in these  
 849 heat fluxes being larger than approximately  $\pm 100 \text{ mW m}^{-2}$ , with a net imbalance of  
 850  $16 \text{ mW m}^{-2}$ .

851 Under option 2 where  $T_{\text{model}}$  is interpreted as Conservative Temperature, the air-  
852 sea flux imbalance does not arise, but two other inaccuracies arise. First, under option 2  
853 the bulk formulae that determine part of the air-sea flux is based on the surface values of  
854  $\Theta$  rather than of  $\theta$  (for which the bulk formulae are designed). Second, the isobaric  
855 density gradient in the upper ocean is typically different by ~1% to the isobaric density  
856 gradient that would be found if the TEOS-10 equation of state had been adopted in these  
857 models. These two aspects of option 2 are considered less serious than not conserving  
858 heat at the sea surface by up to  $\pm 100 \text{ mW m}^{-2}$ . Neither of the two inaccuracies that arise  
859 under option 2 are fundamental thermodynamic errors. Rather they are equivalent to  
860 the ocean modeler choosing (i) a slightly different bulk formulae, and (ii) a slightly  
861 different equation of state. The constants in the bulk formulae are very poorly known so  
862 that the switching from  $\theta$  to  $\Theta$  in their use will be well within their uncertainty (Cronin  
863 et al., 2019) while the ~1% change to the isobaric density gradient due to using the  
864 different equations of state is at the level of our knowledge of the equation of state of sea  
865 water (see the discussion section below).

866 We conclude that option 2 where the  $T_{\text{model}}$  in EOS-80 models is interpreted as  
867 Conservative Temperature is much preferred as it treats the air-sea heat flux in a manner  
868 consistent with the First Law of Thermodynamics, and the treatment of  $T_{\text{model}}$  as being a  
869 conservative variable in the ocean interior is more consistent with it being Conservative  
870 Temperature than being potential temperature. These same two features of ocean  
871 models mean that  $T_{\text{model}}$  cannot be accurately interpreted as potential temperature, since  
872 both the surface flux boundary condition and the lack of the non-conservative source  
873 terms in the ocean interior mean that these ocean models continually force  $T_{\text{model}}$  away  
874 from being potential temperature, even if it was initialized as such.

875

## 876 5. Comparison with ocean observations

877 Now that we have argued that  $T_{\text{model}}$  of EOS-80 based models should be  
878 interpreted as being Conservative Temperature, how then should the model-based  
879 estimates of ocean heat content and ocean heat flux be compared with ocean  
880 observations and ocean atlas data? The answer is by evaluating the ocean heat content

881 correctly in the observed data sets using TEOS-10, whereby the observed data is used to  
882 calculate Conservative Temperature, and this is used together with  $c_p^0$  to evaluate ocean  
883 heat content and meridional heat fluxes.

884 We have made the case that the salinity variable in CMIP ocean models that have  
885 been spun up for several centuries is Preformed Salinity  $S_*$  for the TEOS-10 compliant  
886 models, and is  $S_*/u_{ps}$  for the EOS-80 compliant models. Hence it is the value of either  
887  $S_*$  or  $S_*/u_{ps}$  calculated from ocean observations to which the model salinities should be  
888 compared. Preformed Salinity  $S_*$  is different to Reference Salinity  $S_R$  by only the ratio  
889  $0.26 = 0.35/1.35$  compared with the difference between Absolute Salinity and Preformed  
890 Salinity (see Figure 4), and these differences are generally only significantly different to  
891 zero at depths exceeding 500 m. Note that Preformed Salinity can be evaluated from  
892 observations of Practical Salinity using the Gibbs SeaWater (GSW) software  
893 `gsw_Sstar_from_SP`.

894

## 895 6. Discussion and Recommendations

896 We have made the case that it is advisable to avoid non-conservative sources of  
897 heat at the sea surface. It is the prior interpretation of the temperature variable in EOS-  
898 80 based models as being potential temperature that implies that the ocean receives a  
899 heat flux that is larger by  $\Delta Q$  than the heat that is lost from the atmosphere. Since there  
900 are some areas of the ocean surface where  $\Delta Q$  is as large as the mean rate of global  
901 warming, the issue is important in practice. This realization has motivated the new  
902 interpretation of the prognostic temperature of EOS-80 ocean models as being  
903 Conservative Temperature (our option 2, section 4.2).

904 A consequence of this new interpretation of the prognostic temperature variable  
905 of all CMIP ocean models as being Conservative Temperature means that the EOS-80  
906 based models suffer a relative error of  $\sim 1\%$  in their isobaric gradient of *in situ* density in  
907 the warm upper ocean. How worried should we be about this error? One perspective  
908 on this question is to simply note (from above) that there are larger relative errors  
909 ( $\sim 2.7\%$ ) in the thermal wind equation in the deep ocean due to the neglect of variations  
910 in the relative composition of sea salt. Another perspective is to ask how well science

911 even knows the thermal expansion coefficient, for example. From appendices K and O  
912 of IOC et al. (2010) (and section 7 of McDougall and Barker (2011)) we see that the RMS  
913 value of the differences between the individual laboratory-based data points of the  
914 thermal expansion coefficient and the thermal expansion coefficient obtained from the  
915 fitted TEOS-10 Gibbs function is  $0.73 \times 10^{-6} \text{ K}^{-1}$  which is approximately 0.5% of a typical  
916 value of the thermal expansion coefficient in the ocean. Without a proper estimation of  
917 the number of degrees of freedom represented by the fitted data points, we might  
918 estimate the relative error of the thermal expansion coefficient obtained from the fitted  
919 TEOS-10 Gibbs function as being half of this, namely 0.25%. So a typical relative error in  
920 the isobaric density gradient of  $\sim 1\%$  in the upper ocean due to using  $\Theta$  rather than  $\theta$  as  
921 the temperature input seems undesirable but not serious.

922 We must also acknowledge that all models have ignored the difference between  
923 Prefomed Salinity, Reference Salinity and Absolute Salinity (which is the salinity  
924 variable from which density is accurately calculated). As discussed in IOC et al. (2010),  
925 Wright et al. (2011) and McDougall and Barker (2011), glossing over these issues of the  
926 spatially variable composition of sea salt, which is the same as glossing over the effects  
927 of biogeochemistry on salinity and density, means that all our ocean and climate models  
928 have errors in their thermal wind (vertical shear of horizontal velocity) that globally  
929 exceed 2.7% for half the ocean volume deeper than 1000 m. In the deep North Pacific  
930 Ocean, the misestimation of thermal wind is many times this 2.7% value. The  
931 recommended way of incorporating the spatially varying composition of seawater into  
932 ocean models appears as section A.20 in the TEOS-10 Manual (IOC et al. (2010)), and as  
933 section 9 in the McDougall and Barker (2012), with ocean models needing to carry a  
934 second salinity type variable. While it is true that this procedure has the effect of  
935 relaxing the model towards the non-standard seawater composition of today's ocean, it  
936 is clearly advantageous to make a start with this issue by incorporating the non-  
937 conservative source terms that apply to the present ocean rather than to continue to  
938 ignore the issue altogether. As explained in these references, once the modelling of  
939 ocean biogeochemistry matures, the difference between the various types of salinity can

940 be calculated in real time in an ocean model without the need of referring to historical  
941 data.

942         Nevertheless, we acknowledge that no published ocean model to date has  
943 attempted to include the influence of biogeochemistry on salinity and density, and  
944 therefore we recommend that the salinity from both observations and model output be  
945 treated as Preformed Salinity  $S_p$ .

946

#### 947 *6.1 Contrasts to the recommendations of Griffies et al. (2016)*

948         How does this paper differ from the recommendations in Griffies et al. (2016)?  
949 That paper recommended that the ocean heat content and meridional transport of heat  
950 should be calculated using the model's temperature variable and the model's value of  
951  $c_p^0$ , and we strenuously agree. However, in the present paper we argue that the  
952 temperature variable carried by an EOS-80 based ocean model should be interpreted as  
953 being Conservative Temperature, and not be interpreted as being potential temperature.  
954 This idea was raised as a possibility in Griffies et al. (2016), but the issue was left unclear  
955 in that paper. For example, section D2 of Griffies et al. (2016) recommends that TEOS-10  
956 based models archive potential temperature (as well as their model variable,  
957 Conservative Temperature) "in order to allow meaningful comparisons" with the output  
958 of the EOS-80 based models. We now disagree with this suggestion; the thesis of the  
959 present paper is that the temperature variables of both EOS-80 and TEOS-10 based  
960 models are already directly comparable, and they should both be interpreted as being  
961 Conservative Temperature, and they should both be compared with Conservative  
962 Temperature from observations. The fact that the model's temperature variable is  
963 labelled "thetao" in EOS-80 models and "bigthetao" in TEOS-10 based models we now  
964 see as very likely to cause confusion, since we are recommending that the temperature  
965 outputs of both types of ocean models should be interpreted as Conservative  
966 Temperature.

967         The present paper also diverges from Griffies et al. (2016) in the way that the  
968 salinity variables in CMIP ocean models should be interpreted and thus compared to  
969 observations. Griffies et al. (2016) interpret the salinity variable in TEOS-10 based ocean



970 models as being Reference Salinity  $S_R$  whereas we show that these models actually  
 971 carry Preformed Salinity  $S_*$  but have errors in their calculation of densities. Similarly,  
 972 Griffies et al. (2016) interpret the salinity variable in EOS-80 based ocean models as being  
 973 Practical Salinity  $S_p$  whereas we show that these models actually carry  $S_*/u_{ps}$ , that is,  
 974 Preformed Salinity divided by the constant,  $u_{ps}$ . This distinction between the present  
 975 paper and Griffies et al. (2016) is negligible in the upper ocean where Preformed Salinity  
 976 is almost identical to Reference Salinity (because the composition of seawater in the  
 977 upper ocean is close to Reference Composition), but in the deeper parts of the ocean, the  
 978 distinction is not negligible; for example, based on the work of McCarthy et al. (2015) we  
 979 have shown that the use of Absolute Salinity versus Preformed Salinity leads to  $\sim 1$  Sv  
 980 difference in the meridional overturning streamfunction in the North Atlantic at a depth  
 981 of 2700 m. However, in this deeper part of the ocean, even though the difference  
 982 between Absolute Salinity and Preformed Salinity is not negligible, the difference  
 983 between Preformed Salinity and Reference Salinity (which the TEOS-10 based ocean  
 984 models have to date assumed their salinity variable to be) is smaller in the ratio  $0.35/1.35$   
 985  $= 0.26$  (see Figure 4). That is, if the salinity output of a TEOS-10 based ocean model was  
 986 taken to be Reference Salinity, the error would be only a quarter of the difference  
 987 between Absolute Salinity and Preformed Salinity, a difference which limits the  
 988 accuracy of the isobaric density gradients in the deeper parts of ocean models (see  
 989 Figure 4). A similar remark applies to EOS-80 based ocean models if their salinity  
 990 output is regarded as being Practical Salinity instead of being (as we propose)  $S_*/u_{ps}$ .

991

992

### 993 **6.2 Summary table of ocean heat content imbalances**

994 In Table 1 we summarize the effects of uncertainties in physical or numerical processes  
 995 in estimating ocean heat content or its changes. The first two rows are the rate of  
 996 warming (expressed in  $\text{mWm}^{-2}$  averaged over the sea surface) due to anthropogenic  
 997 global warming, and due to geothermal heating. The third row is an estimate of the  
 998 surface heat flux equivalent of the depth-integrated rate of dissipation of turbulent  
 999 kinetic energy, and the fourth is an estimate of the neglected net flux of potential

1000 enthalpy at the sea surface due to the evaporation and precipitation of water occurring  
1001 at different temperatures.

1002 The next (fifth) row is the consequence of considering the scenario where all the  
1003 radiant heat is absorbed into the ocean at a pressure of 25 dbar rather than at the sea  
1004 surface. The derivative of specific enthalpy with respect to Conservative Temperature at  
1005 25 dbar,  $\hat{h}_\theta$ , is  $c_p^0$  times the ratio of the absolute in situ temperature at 25 dbar,  $(T_0 + t)$ ,  
1006 to the absolute potential temperature,  $(T_0 + \theta)$  at this pressure (see Eqn. (A.11.15) of IOC  
1007 et al. (2010)). The ratio of  $\hat{h}_\theta$  to  $c_p^0$  at 25 dbar is typically different to unity by  $6 \times 10^{-6}$ ,  
1008 and taking a typical rate of radiative heating of  $100 \text{ Wm}^{-2}$  over the ocean's surface leads  
1009 to  $0.6 \text{ mWm}^{-2}$  as the area-averaged rate of mis-estimation of the surface flux of  
1010 Conservative Temperature for this assumed pressure of penetrative radiation. Since this  
1011 is so small, the use of  $c_p^0$  (rather than  $\hat{h}_\theta$ ) to convert the divergence of the radiative heat  
1012 flux into a flux of Conservative Temperature is well supported, providing the correct  
1013 diagnostics are used for the calculation (such diagnostic issues may be responsible for  
1014 the heat budget closure issues identified by Irving et al. 2020).

1015 The next six rows of Table 1 list the mean and twice the standard deviation of the  
1016 volume integrated non-conservative production of Conservative Temperature, potential  
1017 temperature, and specific entropy, all expressed in  $\text{mWm}^{-2}$  at the sea surface. The  
1018 following two rows are the results we have found in this paper for the air-sea heat flux  
1019 error that is made if the EOS-80's temperature is taken to be potential temperature.

1020 The final three rows show that ocean models, being cast in flux divergence form  
1021 with heat fluxes being passed between one grid box and the next, do not have  
1022 appreciable numerical errors in deducing air-sea fluxes from changes in the volume  
1023 integrated heat content.

1024 The estimate from Graham and McDougall (2013) of  $-10 \text{ mWm}^{-2}$  is for the net  
1025 interior production of  $\theta$ , so this is a net destruction. A steady state requires this amount  
1026 of extra flux of  $\theta$  at the sea surface (so it can be consumed in the interior). Our estimate  
1027 of this extra flux of  $\theta$  at the sea surface is  $16 \text{ mWm}^{-2}$ , which is only a little larger than the  
1028 estimate of Graham and McDougall (2013).

1029

1030 **6.3 Summary of recommendations**

1031 In summary, this paper has argued for the following guidelines for analyzing the  
1032 CMIP model runs. We should

- 1033 1. interpret the prognostic temperature variable of all CMIP models (whether they  
1034 are based on the EOS-80 or the TEOS-10 equation of state) as being Conservative  
1035 Temperature,
- 1036 2. compare the model's prognostic temperature with the Conservative  
1037 Temperature,  $\Theta$ , of observational data,
- 1038 3. calculate the ocean heat content as the volume integral of the product of  
1039 (i) in situ density (for non-Boussinesq models or reference density for  
1040 Boussinesq) (ii) the model's prognostic temperature,  $\Theta$ , and (iii) the model's  
1041 value of  $c_p^0$ ,
- 1042 4. interpret the salinity variable of the model output as being Prefomed Salinity  $S_*$   
1043 for TEOS-10 based ocean models, and  $S_*/u_{ps}$  for EOS-80 based ocean models (so  
1044 it is advisable to post-multiply the salinity output of EOS-80 models by  $u_{ps}$  in  
1045 order to have the salinity outputs of all types of CMIP models as Prefomed  
1046 Salinity  $S_*$ ) and,
- 1047 5. compare the model's salinity variable with Prefomed Salinity,  $S_*$ , calculated  
1048 from ocean observations.
- 1049 6. Sea surface temperature should be taken as the model's prognostic temperature  
1050 in the case of EOS-80 models (since this is the temperature that was used in the  
1051 bulk formulae), and as the calculated and stored values of potential temperature  
1052 in the case of TEOS-10 models.
- 1053 7. Ensure that all required fixed variables, such as  $c_p^0$ , (boussinesq) reference  
1054 density, seawater volume, and freezing equation are saved to the CMIP archives  
1055 alongside the prognostic temperature and salinity variables, so that analysts have  
1056 all components required to accurately interpret the model fields. In addition,  
1057 providing the full-depth OHC timeseries for each simulation would provide a  
1058 quantified target for analysts to compare and contrast changes across models and  
1059 simulations.

1060 Note that this sixth recommendation for EOS-80 based models exposes an unavoidable  
1061 inconsistency in that the surface values of the model's prognostic temperature is best  
1062 regarded internally in the ocean model as being Conservative Temperature, but we  
1063 cannot avoid the fact that this same temperature was used as the sea surface (*in situ*)  
1064 temperature in the bulk formulae during the running of such ocean models. Issues such  
1065 as these will not arise when all ocean models have been converted to the TEOS-10  
1066 equation of state.

1067 How then should the model's salinity and temperature outputs,  $S_s$  and  $\Theta$ , be used to  
1068 evaluate dynamical concepts such as streamfunctions, dynamic height, etc? The answer  
1069 most consistent with the running of a numerical model is to use the equation of state  
1070 that the model used, together with the model's temperature and salinity outputs on the  
1071 native grid of the model. This method is important when studying detailed dynamical  
1072 balances in ocean model output. But since we now have the output salinity and  
1073 temperature of both EOS-80 and TEOS-10 models being the same (namely  $S_s$  and  $\Theta$ ),  
1074 there is an efficiency and simplicity argument to analyze the output of all these models  
1075 in the same manner, using algorithms from the Gibbs SeaWater (GSW) Oceanographic  
1076 Toolbox of TEOS-10 (McDougall and Barker, 2011). Doing these model inter-  
1077 comparisons often involves interpolating the model outputs to different depths (or  
1078 pressures) than those used in the original ocean model, so incurring some interpolation  
1079 errors. While the use of the GSW software means that the *in situ* density will be  
1080 calculated slightly differently than in some of the forward models, thus affecting the  
1081 thermal wind and sea-level rise, these differences are small, as can be seen by comparing  
1082 Figures A.5.1 and A.5.2 of the TEOS-10 Manual, IOC et al. (2010). Hence we think that it  
1083 is viable for most purposes to evaluate density and dynamic height using the GSW  
1084 Oceanographic Toolbox, with the input salinity to this GSW code being the model's  
1085 Preformed Salinity, and the temperature input being the Conservative Temperature,  
1086 which as we have argued, are the model's prognostic salinity and temperature variables.

1087 Another issue that may arise is where a TEOS-10 based model has been run with  
1088 Conservative Temperature, but the monthly-mean Conservative Temperature output  
1089 has been converted into potential temperature before sending the model output to the

1090 CMIP archive. What is the damage done if this inaccurately averaged value of potential  
1091 temperature is converted back to Conservative Temperature using only the monthly-  
1092 mean potential temperature and salinity? While such an issue is perhaps an operational  
1093 detail that takes us some distance from our intention of writing an academic paper about  
1094 these issues, nevertheless we show Figure 9 which indicates that transforming between  
1095 these monthly-averaged values is not a serious issue for relatively coarse-resolution  
1096 ocean models.

1097

#### 1098 **Author Contribution**

1099 T J McD. devised this new way of interpreting CMIP ocean model variables, P. M. B and  
1100 R. M. H. provided figures for the paper, and all authors contributed to the concepts and  
1101 the writing of the manuscript.

1102

1103 **Acknowledgements.** We have benefitted from comments and suggestions from Drs.  
1104 Baylor Fox-Kemper, Sjoerd Groeskamp, Casimir de Lavergne, John Krasting, Fabien  
1105 Roquet, Geoff Stanley, Jan-Erik Tesdal, R. Feistel and R. Tailleux. This paper contributes  
1106 to the tasks of the Joint SCOR/IAPSO/IAPWS Committee on the Thermophysical  
1107 Properties of Seawater. T. J. McD., P. M. B. and R. M. H. gratefully acknowledge  
1108 Australian Research Council support through grant FL150100090. The work of P.J.D.  
1109 was prepared by Lawrence Livermore National Laboratory (LLNL) under contract no.  
1110 DE-AC52-07NA27344.

1111

1112 **Appendix A: A non-seawater thermodynamic interpretation of Option 1**

1113 Ocean models have always assumed a constant isobaric heat capacity and have  
 1114 traditionally assumed that the model's temperature variable is whatever temperature  
 1115 the equation of state was designed to accept. Here we enquire whether there is a way of  
 1116 justifying Option 1 thermodynamically in the sense that Option 1 would be totally  
 1117 consistent with thermodynamic principles for a fluid that is different to real seawater.

1118 That is, we pursue the idea that these EOS-80 based ocean models are not  
 1119 actually models of seawater but are models of a slightly different fluid. We require a  
 1120 fluid that is identical to seawater in some respects, such as that it has the same dissolved  
 1121 material (Millero et al., 2008) and the same issues around Absolute Salinity, Prefomed  
 1122 Salinity and Practical Salinity, and the same in situ density as real seawater (at given  
 1123 values of Absolute Salinity, potential temperature and pressure). But we require that the  
 1124 expression for the enthalpy of this new fluid is different to that of real seawater.

1125 The difference that we envisage between real seawater and this new fluid is that,  
 1126 at zero pressure, the enthalpy of the new fluid is given exactly by the constant value  $c_p^0$   
 1127 times potential temperature  $\theta$ . That is, for the new fluid, potential enthalpy  $h^0$  is  
 1128 simply  $c_p^0\theta$  (as it would be for an ideal gas), and the air-sea interaction for this new fluid  
 1129 would be exactly as it occurs in the EOS-80 based models. Moreover, conservation of  
 1130 potential temperature is justified for this new fluid, and the density and thermal wind  
 1131 would also be correctly evaluated in these EOS-80 based models.

1132 The enthalpy of this new fluid is then given by (since  $h_p = v$ )

$$1133 \quad \bar{h}(S_A, \theta, p) = c_p^0 \theta + \int_{p_0}^p \bar{v}(S_A, \theta, p') dp', \quad (A1)$$

1134 while the entropy of this new fluid needs to obey the consistency relationship,

1135  $\bar{\eta}_\theta = \bar{h}_\theta(p=0)/(T_0 + \theta)$ , which reduces to

$$1136 \quad \bar{\eta}_\theta = \frac{c_p^0}{(T_0 + \theta)}, \quad (A2)$$

1137 where  $T_0 = 273.15$  K is the Celsius zero point. This consistency relationship is derived  
 1138 directly from the Fundamental Thermodynamic Relationship (see Table P.1 of IOC et al.,

1139 2010). Integrating Eqn. (A2) with respect to potential temperature at constant salinity  
 1140 leads to the following expression for entropy that our new fluid must obey,

$$1141 \quad \bar{\eta}(S_A, \theta) = c_p^0 \ln\left(1 + \frac{\theta}{T_0}\right) + a \left(\frac{S_A}{S_{SO}}\right) \ln\left(\frac{S_A}{S_{SO}}\right). \quad (\text{A3})$$

1142 The variation here with salinity is taken from the TEOS-10 Gibbs-function-derived  
 1143 expression for specific entropy which contains the last term in Eqn. (A3) with the  
 1144 coefficient  $a$  being  $a = -9.310292413479596 \text{ J kg}^{-1} \text{ K}^{-1}$  (this is the value of the coefficient  
 1145 derived from the  $g_{110}$  coefficient of the Gibbs function (appendix H of IOC *et al.* (2010)),  
 1146 allowing for our version of the normalization of salinity,  $(S_A/S_{SO})$ ). This term was  
 1147 derived by Feistel (2008) to be theoretically correct at vanishingly small Absolute  
 1148 Salinities.

1149 With these definitions, Eqns. (A1) and (A3), of enthalpy and entropy of our new  
 1150 fluid, we have completely defined all the thermophysical properties of the fluid (see  
 1151 Appendix P of IOC *et al.*, 2010 for a discussion). Many aspects of the fluid are different  
 1152 to seawater, including the adiabatic lapse rate (and hence the relationship between in  
 1153 situ and potential temperatures), since the adiabatic lapse rate is given by  $\Gamma = \tilde{h}_{\theta p} / \tilde{\eta}_{\theta}$   
 1154 and while the numerator is the same as for seawater (since  $\tilde{h}_{\theta p} = \tilde{h}_{\theta p} = \tilde{v}_{\theta}$ ), the  
 1155 denominator,  $\tilde{\eta}_{\theta}$ , which is now given by Eqn. (A2), can be up to 6% different to the  
 1156 corresponding function,  $\tilde{\eta}_{\theta}$ , appropriate to real seawater.

1157 We conclude that this is indeed a conceptual way of forcing the EOS-80 based  
 1158 models to be consistent with thermodynamic principles. That is, we have shown that  
 1159 these EOS-80 models are not models of seawater, but they do accurately model a  
 1160 different fluid whose thermodynamic definition we have given in Eqns. (A1) and (A3).  
 1161 This new fluid interacts with the atmosphere in the way that EOS-80 models have  
 1162 assumed to date, the potential temperature of this new fluid is correctly mixed in the  
 1163 ocean in a conservative fashion, and the equation of state is written in terms of the  
 1164 model's temperature variable, namely potential temperature.

1165 Hence we have constructed a fluid which is different thermodynamically to  
 1166 seawater, but it does behave exactly as these EOS-80 models treat their model seawater.  
 1167 That is, we have constructed a new fluid which, if seawater had these thermodynamic

1168 characteristics, then the EOS-80 ocean models would have correct thermodynamics,  
1169 while being able to interpret the model's temperature variable as being potential  
1170 temperature.

1171         But this does not change the fact that in order to make these EOS-80 models  
1172 thermodynamically consistent in this way we have ignored the real variation at the sea  
1173 surface of the isobaric specific heat capacity; a variation that we know can be as large as  
1174 6%.

1175         Hence we do not propose this non-seawater explanation as a useful  
1176 rationalization of the behaviour of EOS-80 based ocean models. Rather, it seems less  
1177 dramatic and more climatically relevant to adopt the simpler interpretation of Option 2.  
1178 Under this option we accept that the model is modelling actual seawater, that the  
1179 model's temperature variable is in fact Conservative Temperature, and that there are  
1180 some errors in the equation of state of these EOS-80 models that amount to errors of the  
1181 order of 1% in the thermal wind relation throughout much of the upper (warm) ocean.  
1182 That is, so long as we interpret the temperature variable of these EOS-80 based models  
1183 as Conservative Temperature, they are fine except that they have used an incorrect  
1184 equation of state; they have used  $\bar{\rho}$  rather than  $\hat{\rho}$ . Apart from this "error" in the ocean  
1185 code, Option 2 is a consistent interpretation of the ocean model thermodynamics and  
1186 dynamics. In ocean models there are always questions of how to parameterize ocean  
1187 mixing. To this uncertain aspect of ocean physics, under Option 2 we add the less than  
1188 desirable expression that is used to evaluate density in EOS-80 based ocean models in  
1189 CMIP

1190

1191



1192 **Appendix B: An alternative derivation of Eqn. (10)**

1193 Eqn. (10) is an expression for the error in the isobaric density gradient when  
 1194 Conservative Temperature is used as the input temperature variable to the EOS-80  
 1195 equation of state (which expects its input temperature to be potential temperature). An  
 1196 alternative accurate expression to Eqn. (9) for the isobaric density gradient is

$$1197 \quad \tilde{\rho}_{S_*} \nabla_p S_* + \tilde{\rho}_\theta \nabla_p \theta, \quad (\text{B1})$$

1198 and subtracting this from the incorrect expression, Eqn. (8), gives the following  
 1199 expression for the model's error in evaluating the isobaric gradient of in situ density,

$$1200 \quad \text{error in } \nabla_p \rho = \tilde{\rho}_\theta \nabla_p (\Theta - \theta). \quad (\text{B2})$$

1201 An approximate fit to the temperature difference,  $\Theta - \theta$ , as displayed in Figure 2 is

$$1202 \quad (\Theta - \theta) \approx 0.05 \Theta \left( 1 - \frac{S_A}{S_{SO}} \right) - 1.75 \times 10^{-3} \Theta \left( 1 - \frac{\Theta}{25^\circ\text{C}} \right), \quad (\text{B3})$$

1203 and using this approximate expression in the right-hand side of Eqn. (B2) gives

$$1204 \quad \frac{\text{error in } \nabla_p \rho}{\tilde{\rho}_\theta} \approx \left[ 0.05 \left( 1 - \frac{S_A}{S_{SO}} \right) - 1.75 \times 10^{-3} \left( 1 - \frac{\Theta}{12.5^\circ\text{C}} \right) \right] \nabla_p \Theta - \frac{0.05}{S_{SO}} \Theta \nabla_p S_*. \quad (\text{B4})$$

1205 The first part of this expression that multiplies  $\nabla_p \Theta$  corresponds to the proportional  
 1206 error in the thermal expansion coefficient displayed in Figure 7(a). The second part of  
 1207 Eqn. (B4) amounts to an error in the saline derivative of the equation of state, with the  
 1208 proportional error (corresponding to Eqn. (12)), being  $-0.05 \tilde{\rho}_\theta \Theta / (\hat{\rho}_{S_A} S_{SO})$ , and this is  
 1209 close to the error that can be seen in Figure 7(b). This error is approximately a quadratic  
 1210 function of temperature since the thermal expansion coefficient  $\tilde{\rho}_\theta$  is approximately a  
 1211 linear function of temperature.

1212

1213

1214

1215  
1216

	Heat flux contributions of different processes	mWm <sup>-2</sup>
Physical processes	Global warming imbalance (Zanna et al., 2019), mean	<b>+300</b>
	Geothermal heating (Emile-Geay and Madec, 2009), mean	<b>+86</b>
	Viscous dissipation (Graham and McDougall, 2013), mean	<b>+3</b>
	Atmospheric water fluxes of enthalpy (Griffies et al. 2016), mean	<b>-(150-300)</b>
Non-conservation errors	Extra flux of $\Theta$ if the air-sea radiative heat flux is taken to occur at a pressure of 25dbar	<b>-0.6</b>
	non-conservation of $\Theta$ (Graham & McDougall 2013), mean	<b>+0.3</b>
	non-conservation of $\Theta$ (Graham & McDougall 2013), 2*rms	<b>+1</b>
	non-conservation of $\theta$ (Graham & McDougall 2013), mean	<b>-10</b>
	non-conservation of $\theta$ (Graham & McDougall 2013), 2*rms	$\pm$ <b>120</b>
	non-conservation of $\eta$ (Graham & McDougall 2013), mean	<b>+380</b>
	non-conservation of $\eta$ (Graham & McDougall 2013), 2*rms	<b>+1200</b>
	Interpreting EOS-80 T as $\theta$ (ACCESS-CM2 estimate), mean	<b>+16</b>
	Interpreting EOS-80 T as $\theta$ (ACCESS-CM2 estimate), 2*rms	$\pm$ <b>135</b>
Numerical errors	ACCESS-OM2 single time-step	$\pm$ <b>10<sup>-7</sup></b>
	ACCESS-OM2 diagnosed from OHC snapshots	$\pm$ <b>0.001</b>
	ACCESS-CM2 diagnosed from OHC monthly-averages	$\pm$ <b>0.03</b>

1217  
1218  
1219  
1220  
1221  
1222  
1223  
1224  
1225  
1226

**Table 1:** Summary of the impact of various processes and modelling errors on the global ocean heat budget and its imbalance. All numbers are in units of mWm<sup>-2</sup>. Numerical errors are diagnosed from either ACCESS-OM2 (machine precision errors) or ACCESS-CM2 (associated with not having access to OHC snapshots). Numbers from interior processes are converted to equivalent surface fluxes by depth integration. The sign convention here is that a positive heat flux is heat entering the ocean or warming the ocean by internal dissipation. The symbol  $\eta$  in this table stands for entropy.

1227 **Code Availability**

1228 This paper has not run any ocean or climate models, and so has not produced any  
1229 such computer code. Processed data and code to produce the ACCESS-CM2 figures 5,  
1230 6 and 9 is located at the github repository

1231 [https://github.com/rmholmes/ACCESS\\_CM2\\_SpecificHeat](https://github.com/rmholmes/ACCESS_CM2_SpecificHeat).

1232

1233

1234 **Data Availability**

1235 This paper has not produced any model data. Processed data and code to produce the  
1236 ACCESS-CM2 figures 5, 6 and 9 is located at the github repository

1237 [https://github.com/rmholmes/ACCESS\\_CM2\\_SpecificHeat](https://github.com/rmholmes/ACCESS_CM2_SpecificHeat).

1238

1239

1240

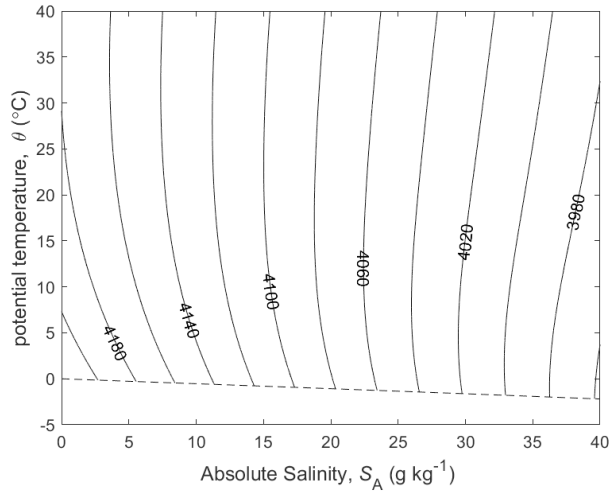
1241 **References**

- 1242 Bi, D., Dix, M., Marsland, S., O'Farrell, S., Rashid, H., Uotila, P., Hirst, A., Kowalczyk, E.,  
 1243 Golebiewski, M., Sullivan, A., Yan, H., Hannah, N., Franklin, C., Sun, Z., Vohralik, P.,  
 1244 Watterson, I., Zhou, X., Fiedler, R., Collier, M., Ma, Y., Noonan, J., Stevens, L., Uhe, P.,  
 1245 Zhu, H., Griffies, S., Hill, R., Harris, C. and Puri, K.: The ACCESS coupled model:  
 1246 description, control climate and evaluation, *Aust. Met. Oceanogr. J.*, **63**, 41-64, 2013.
- 1247 Cronin M. F., Gentemann C. L., Edson J, Ueki I., Bourassa M., Brown S., Clayson C. A.,  
 1248 Fairall C. W., Farrar J. T., Gille S. T., Gulev S., Josey S. A., Kato S., Katsumata M., Kent  
 1249 E., Krug M., Minnett P. J., Parfitt R., Pinker R. T., Stackhouse P. W., Swart S., Tomita H.,  
 1250 Vandemark D., Weller A. R., Yoneyama K., Yu L., Zhang D.: Air-Sea Fluxes With a  
 1251 Focus on Heat and Momentum. *Frontiers in Marine Science*, **6**, 430.  
 1252 <https://www.frontiersin.org/article/10.3389/fmars.2019.00430> , 2019.
- 1253 Emile-Geay J. and Madec G.: Geothermal heating, diapycnal mixing and abyssal circulation.  
 1254 *Ocean Science*, **5**, 203-217, 2019.
- 1255 Feistel, R.: A Gibbs function for seawater thermodynamics for -6 to 80 °C and salinity up to  
 1256 120 g kg<sup>-1</sup>, *Deep-Sea Res. I*, **55**, 1639-1671, 2008.
- 1257 Feistel, R., Wright D. G., Kretzschmar H.-J., Hagen E., Herrmann S. and Span R.:  
 1258 Thermodynamic properties of sea air. *Ocean Science*, **6**, 91–141. [http://www.ocean-](http://www.ocean-sci.net/6/91/2010/os-6-91-2010.pdf)  
 1259 [sci.net/6/91/2010/os-6-91-2010.pdf](http://www.ocean-sci.net/6/91/2010/os-6-91-2010.pdf) , 2010.
- 1260 Graham, F. S. and McDougall T. J.: Quantifying the non-conservative production of  
 1261 Conservative Temperature, potential temperature and entropy. *Journal of Physical*  
 1262 *Oceanography*, **43**, 838-862. <http://dx.doi.org/10.1175/JPO-D-11-0188.1> , 2013.
- 1263 Griffies, S. M., Danabasoglu, G., Durack, P. J., Adcroft, A. J., Balaji, V., Böning, C. W.,  
 1264 Chassignet, E. P., Curchitser, E., Deshayes, J., Drange, H., Fox-Kemper, B., Gleckler, P.  
 1265 J., Gregory, J. M., Haak, H., Hallberg, R. W., Heimbach, P., Hewitt, H. T., Holland, D.  
 1266 M., Ilyina, T., Jungclaus, J. H., Komuro, Y., Krasting, J. P., Large, W. G., Marsland, S. J.,  
 1267 Masina, S., McDougall, T. J., Nurser, A. J. G., Orr, J. C., Pirani, A., Qiao, F., Stouffer, R.  
 1268 J., Taylor, K. E., Treguier, A. M., Tsujino, H., Uotila, P., Valdivieso, M., Wang, Q.,  
 1269 Winton, M., and Yeager, S. G.: OMIP contribution to CMIP6: experimental and  
 1270 diagnostic protocol for the physical component of the Ocean Model Intercomparison

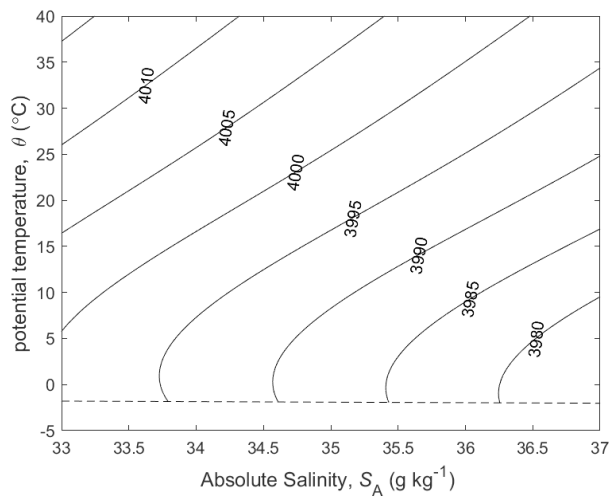
- 1271 Project: *Geosci. Model Dev.*, **9**, 3231-3296, doi:10.5194/gmd-9-3231-2016.  
1272 <http://dx.doi.org/10.5194/gmd-9-3231-2016> , 2016.
- 1273 IOC, SCOR and IAPSO: *The international thermodynamic equation of seawater – 2010:*  
1274 *Calculation and use of thermodynamic properties*. Intergovernmental Oceanographic  
1275 Commission, Manuals and Guides No. 56, UNESCO (English), 196 pp. available at  
1276 [http://www.TEOS-10.org/pubs/TEOS-10\\_Manual.pdf](http://www.TEOS-10.org/pubs/TEOS-10_Manual.pdf) Many of the original papers on  
1277 which TEOS-10 is based were published in the following Special Issue of *Ocean Science*,  
1278 [https://os.copernicus.org/articles/special\\_issue14.html](https://os.copernicus.org/articles/special_issue14.html) 2010.
- 1279 Irving, D., Hobbs W., Church J. and Zika J.: A Mass and Energy Conservation Analysis of  
1280 Drift in the CMIP6 Ensemble. *Journal of Climate*, **34**, 3157-3170,  
1281 <https://doi.org/10.1175/JCLI-D-20-0281.1>, 2021.
- 1282 Jackett, D. R. and McDougall T. J.: Minimal adjustment of hydrographic profiles to achieve  
1283 static stability. *Journal of Atmospheric and Oceanic Technology*, **12**, 381-389.  
1284 <https://journals.ametsoc.org/doi/abs/10.1175/1520-0426%281995%29012%3C0381%3A%3E2.0.CO%3B2> , 1995.
- 1285  
1286 <https://doi.org/10.5194/os-17-909-2021>, 2021.  
1287 <https://doi.org/10.5194/os-17-909-2021>, 2021.  
1288 <https://doi.org/10.5194/os-17-909-2021>, 2021.
- 1289 McCarthy, G.D., Smeed, D.A., Johns, W.E., Frajka-Williams, E., Moat, B.I., Rayner, D.,  
1290 Baringer, M.O., Meinen, C.S., Collins, J. and Bryden, H.L.: Measuring the Atlantic  
1291 Meridional Overturning Circulation at 26°N. *Progress in Oceanography*, **130**, 91-111.  
1292 [doi:10.1016/j.pocean.2014.10.006](https://doi.org/10.1016/j.pocean.2014.10.006) , 2015.
- 1293 McDougall, T. J.: Potential enthalpy: A conservative oceanic variable for evaluating heat  
1294 content and heat fluxes. *Journal of Physical Oceanography*, **33**, 945-963.  
1295 <https://journals.ametsoc.org/jpo/article/33/5/945/10023/> , 2003.
- 1296 McDougall T. J. and Barker P. M.: *Getting started with TEOS-10 and the Gibbs Seawater*  
1297 *(GSW) Oceanographic Toolbox*, 28pp, SCOR/IAPSO WG127, ISBN 978-0-646-55621-5.  
1298 available at [http://www.TEOS-10.org/pubs/Getting\\_Started.pdf](http://www.TEOS-10.org/pubs/Getting_Started.pdf) , 2011.

- 1299 McDougall, T. J., Church J. A. and Jackett, D. R.: Does the nonlinearity of the equation  
1300 of state impose an upper bound on the buoyancy frequency? *Journal of Marine*  
1301 *Research*, **61**, 745-764, <http://dx.doi.org/10.1357/002224003322981138> , 2003.
- 1302 McDougall, T. J. and Feistel R.: What causes the adiabatic lapse rate? *Deep-Sea Research I*,  
1303 **50**, 1523-1535. <http://dx.doi.org/10.1016/j.dsr.2003.09.007> , 2003.
- 1304 McDougall, T. J., Jackett D. R., Millero F. J., Pawlowicz R. and Barker P. M.: A global  
1305 algorithm for estimating Absolute Salinity. *Ocean Science*, **8**, 1123-1134.  
1306 <http://www.ocean-sci.net/8/1123/2012/os-8-1123-2012.pdf> , 2012.
- 1307 Millero, F. J., Feistel R., Wright D. G. and McDougall T. J.: The composition of Standard  
1308 Seawater and the definition of the Reference-Composition Salinity Scale. *Deep-Sea*  
1309 *Research-I*, **55**, 50-72. <http://dx.doi.org/10.1016/j.dsr.2007.10.001> , 2008.
- 1310 Pawlowicz, R.: A model for predicting changes in the electrical conductivity, Practical Salinity,  
1311 and Absolute Salinity of seawater due to variations in relative chemical composition. *Ocean*  
1312 *Science*, **6**, 361–378. <http://www.ocean-sci.net/6/361/2010/os-6-361-2010.pdf> , 2010.
- 1313 Pawlowicz, R.: The Absolute Salinity of seawater diluted by riverwater. *Deep-Sea Research I*,  
1314 **101**, 71-79, 2015.
- 1315 Pawlowicz, R., Wright D. G. and Millero F. J.: The effects of biogeochemical processes on  
1316 oceanic conductivity/salinity/density relationships and the characterization of real seawater.  
1317 *Ocean Science*, **7**, 363–387. <http://www.ocean-sci.net/7/363/2011/os-7-363-2011.pdf>, 2011.
- 1318 Pawlowicz, R., McDougall T., Feistel R. and Tailleux R.: An historical perspective on the  
1319 development of the Thermodynamic Equation of Seawater – 2010: *Ocean Sci.*, **8**, 161-  
1320 174. <http://www.ocean-sci.net/8/161/2012/os-8-161-2012.pdf> , 2012.
- 1321 Roquet, F., Madec G., McDougall T. J. and Barker P. M.: Accurate polynomial expressions for  
1322 the density and specific volume of seawater using the TEOS-10 standard. *Ocean*  
1323 *Modelling*, **90**, 29-43. <http://dx.doi.org/10.1016/j.ocemod.2015.04.002> , 2015.
- 1324 Tailleux, R.: Identifying and quantifying nonconservative energy production/destruction terms  
1325 in hydrostatic Boussinesq primitive equation models. *Ocean Modelling*, **34**, 125-136,  
1326 <https://doi.org/10.1016/j.ocemod.2010.05.003> , 2010.

- 1327 Tailleux, R.: Observational and energetics constraints on the non-conservation of  
1328 potential/Conservative Temperature and implications for ocean modelling. *Ocean*  
1329 *Modelling*, **88**, 26-37. <https://doi.org/10.1016/j.ocemod.2015.02.001>, 2015.
- 1330 von Schuckmann, K. et al. Heat stored in the Earth system: where does the energy go? *Earth*  
1331 *Syst. Sci. Data*, **12**, 2013-2041, 2020.
- 1332 Wright, D. G., Pawlowicz R., McDougall T. J., Feistel R. and Marion G. M.: Absolute Salinity,  
1333 “Density Salinity” and the Reference-Composition Salinity Scale: present and future use  
1334 in the seawater standard TEOS-10. *Ocean Sci.*, **7**, 1-26. [http://www.ocean-](http://www.ocean-sci.net/7/1/2011/os-7-1-2011.pdf)  
1335 [sci.net/7/1/2011/os-7-1-2011.pdf](http://www.ocean-sci.net/7/1/2011/os-7-1-2011.pdf), 2011.
- 1336 Young, W.R., Dynamic Enthalpy, Conservative Temperature, and the Seawater Boussinesq  
1337 Approximation, *Journal of Physical Oceanography*, **40**, 394-400,  
1338 doi: 10.1175/2009JPO4294.1, 2010.
- 1339 Zanna L., Khatiwala S., Gregory J. M., Ison, J. and Heimbach P.: Global reconstruction of  
1340 historical ocean heat storage and transport, *Proceedings of the National Academy of*  
1341 *Sciences*, **116**, 1126-1131, 2019.
- 1342  
1343



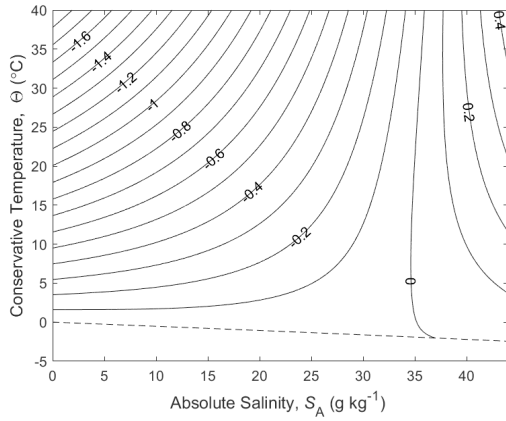
1344



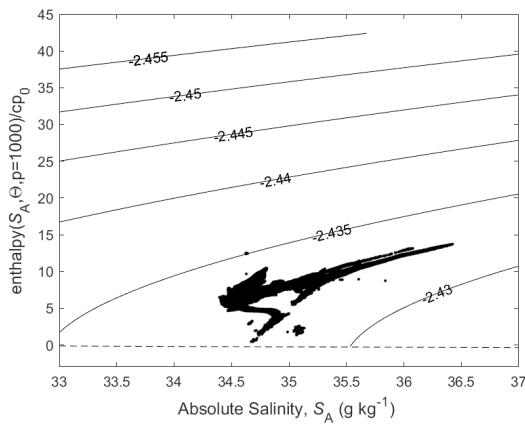
1345  
1346  
1347  
1348  
1349

**Figure 1.** (a) Contours of isobaric specific heat capacity  $c_p$  of seawater (in  $\text{J kg}^{-1} \text{K}^{-1}$ ), at  $p = 0$  dbar. (b) a zoomed-in version for a smaller range of Absolute Salinity. The dashed line is the freezing line at  $p = 0$  dbar.



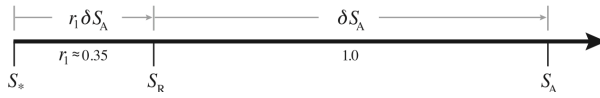


1350  
 1351 **Figure 2.** Contours (in °C) of the difference between potential temperature and  
 1352 Conservative Temperature,  $\theta - \Theta$ .  
 1353  
 1354



1355  
 1356 **Figure 3.** Contours of  $\Theta - \hat{h}(S_A, \Theta, 1000\text{dbar})/c_p^0$  on the Absolute Salinity –  
 1358  $\hat{h}(S_A, \Theta, 1000\text{dbar})/c_p^0$  diagram. Enthalpy,  $\hat{h}(S_A, \Theta, 1000\text{dbar})$ , is a conservative  
 1359 quantity for turbulent mixing processes that occur at a pressure of 1000dbar. The  
 1360 mean value of the contoured quantity is approximately  $-2.44^\circ\text{C}$  illustrating that  
 1361 enthalpy does not possess the “potential” property; that is, enthalpy increases  
 1362 during adiabatic and isohaline increases in pressure. The fact that the contoured  
 1363 quantity on this figure is not a linear function of  $S_A$  and  $\hat{h}(S_A, \Theta, 1000\text{dbar})$   
 1364 illustrates the (small) non-conservative nature of Conservative Temperature. The  
 1365 dots are data from the world ocean at 1000dbar.  
 1366

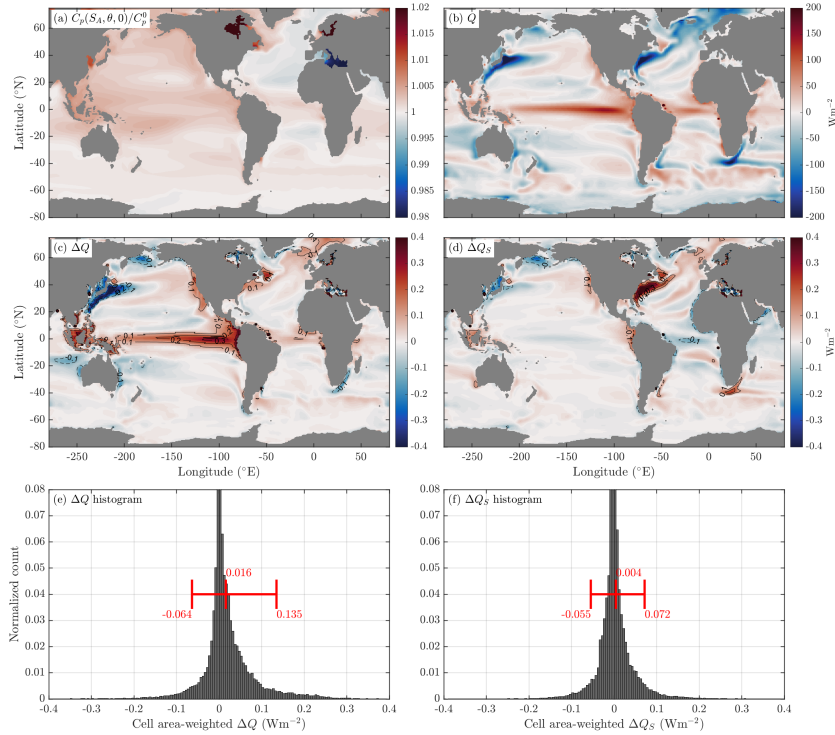
1367  
1368  
1369  
1370



1371  
1372  
1373  
1374  
1375  
1376  
1377  
1378  
1379  
1380

**Figure 4.** Number line of salinity, illustrating the differences between Preformed Salinity  $S_s$ , Reference Salinity  $S_R$ , and Absolute Salinity  $S_A$  for seawater whose composition differs from that of Standard Seawater which has Reference Composition. If a seawater sample has Reference Composition, then  $\delta S_A = 0$  and  $S_s$ ,  $S_R$  and  $S_A$  are all equal.

1381



1382

1383

1384

1385

1386

1387

1388

1389

1390

1391

1392

1393

1394

1395

1396

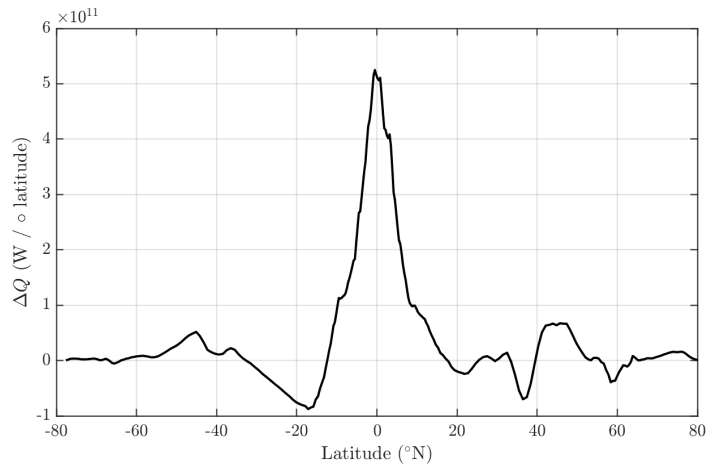
1397

1398

1399

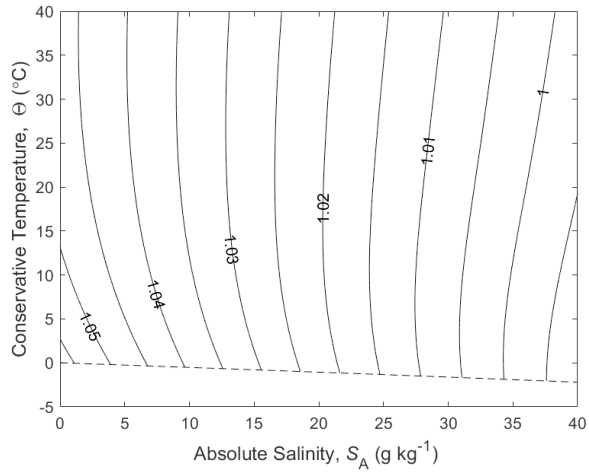
1400

**Figure 5.** (a) The average value of the ratio of the isobaric specific heat of seawater and  $c_p^0$  for data from the ACCESS-CM2 model's pre-industrial control simulation (600 years long). (b) The average surface heat flux  $Q$  ( $\text{Wm}^{-2}$ ) in this same ocean model. (c) The additional heat that the ocean receives/loses compared to the heat that the atmosphere loses/receives (assuming that an EOS-80 model's temperature variable is potential temperature),  $\Delta Q$  ( $\text{Wm}^{-2}$ , Eqn. 6). (e) a histogram of  $\Delta Q$  weighted by the area of each grid cell. (d) The contribution of salinity variations to the air-sea heat flux discrepancy, given by  $\Delta Q_s = Q(S - \bar{S})(1/c_p^0) \partial c_p / \partial S$ , where  $\bar{S}$  is the surface mean salinity and  $\partial c_p / \partial S$  is the variation in the specific heat with salinity at the surface mean salinity and potential temperature. (f) a histogram of  $\Delta Q_s$  weighted by the area of each grid cell. Shown in red in panels e and f are the mean, 5<sup>th</sup> and 95<sup>th</sup> percentiles of the histogram ( $\text{Wm}^{-2}$ ). Note that these calculations neglect correlations between surface properties and the surface heat flux at sub-monthly time scales.

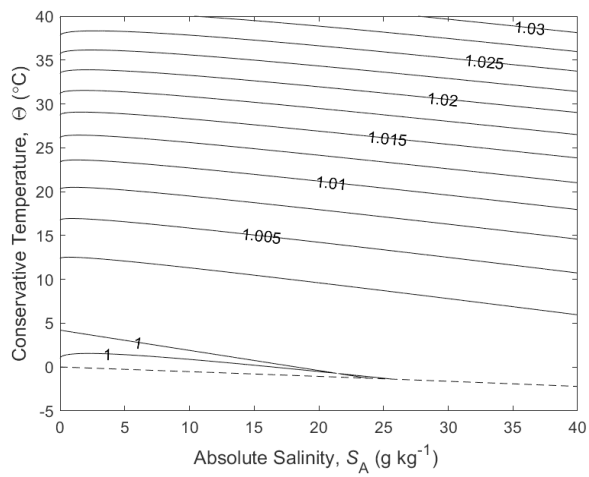


**Figure 6.** The ACCESS-CM2 zonally integrated  $\Delta Q$  From Fig.5c, showing the imbalance in the air-sea heat flux in Watts per degree of latitude.

1401  
1402  
1403  
1404  
1405  
1406



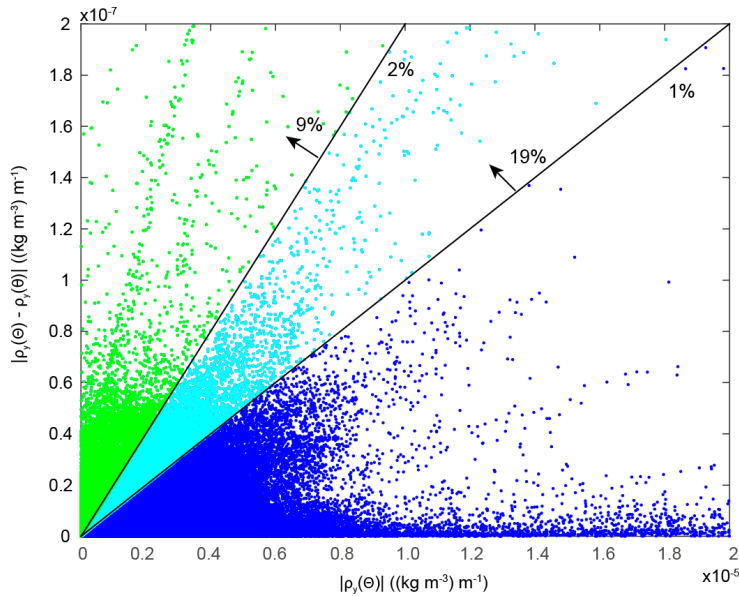
1407

1408  
1409

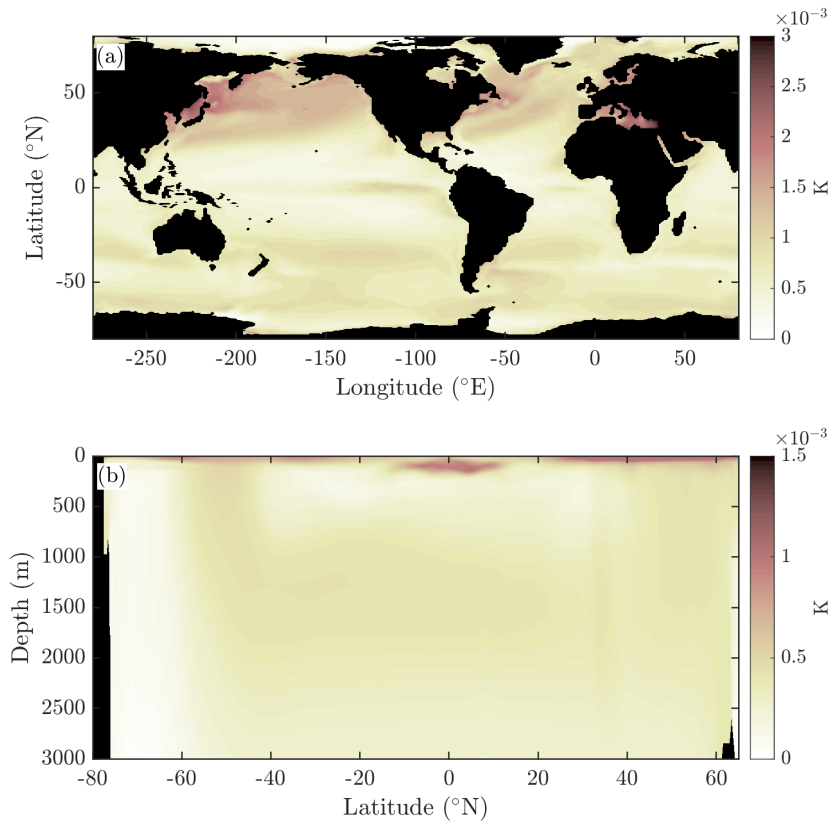
1410 **Figure 7.** (a) The ratio of the thermal expansion coefficients with respect to Conservative  
 1411 Temperature and potential temperature,  $\tilde{\alpha}^\theta/\hat{\alpha}^\theta = \tilde{\Theta}_\theta$ . (b) The ratio of the saline  
 1412 contraction coefficients at constant potential temperature to that at constant Conservative  
 1413 Temperature,  $\tilde{\beta}^\theta/\hat{\beta}^\theta = 1 + (\tilde{\alpha}^\theta/\hat{\beta}^\theta)\hat{\theta}_S/\hat{\theta}_\Theta$  at  $p = 0$  dbar.

1414

1415



1416  
 1417 **Figure 8.** The northward density gradient at constant pressure (the horizontal axis) for  
 1418 data in the global ocean atlas of Gouretski and Koltermann (2004) for  $p < 1000$  dbar. The  
 1419 vertical axis is the magnitude of the difference between evaluating the density gradient  
 1420 using  $\Theta$  versus  $\theta$  as the temperature argument in the expression for density. This is  
 1421 virtually equivalent to the density difference between calling the EOS-80 and the TEOS-10  
 1422 equations of state, using the same numeric inputs for each. The 1% and 2% lines indicate  
 1423 where the isobaric density gradient is in error by 1% and 2%. 19% of the data shallower  
 1424 than 1000 dbar has the isobaric density gradient changed by more than 1% when  
 1425 switching between the equations of state. The median value of the percentage error in the  
 1426 isobaric density gradient is 0.22%.  
 1427  
 1428  
 1429



1430  
1431  
1432  
1433  
1434  
1435  
1436  
1437  
1438  
1439

**Figure 9.** The RMS error (K) in evaluating Conservative Temperature from the CMIP6 archived monthly-averaged values of potential temperature and salinity, compared with averaging the instantaneous values of Conservative Temperature for a month at the (a) surface and (b) the zonal mean. These quantities are calculated from 50 years of temporally averaged output from the ACCESS-CM2 model's pre-industrial control simulation. The errors are seen to be no larger than a few mK.